Plant U-Box 4 regulates chloroplast stress signaling and programmed cell death via Salicylic acid modulation

Snigdha Rai[1], Matthew D. Lemke[1], Anika M. Arias[1], Maria F. Gomez Mendez[2], Katayoon Dehesh[2], and Jesse D. Woodson[1*]

ORCID: SR, 0000-0003-3428-8746; MDL, 0000-0002-9680-0656; AMA, 0009-0008-8025-4153; MFG-M, 0000-0002-2107-5875; KD, 0000-0002-9312-8032; JDW, 0000-0002-5463-5146

[1]The School of Plant Sciences, University of Arizona, Tucson, AZ
[2]Department of Botany and Plant Sciences, Institute for Integrative Genome Biology, University of California, Riverside, CA

[*]Address correspondence to:
Dr. Jesse D. Woodson
303 Forbes Hall
1140 E. South Campus Drive
University of Arizona
Tucson, AZ 85721-0036
Phone: (520) 621-3970
jessewoodson@arizona.edu

Current email addresses: SR: snigdharai@arizona.edu, MDL: matthewlemke@arizona.edu, AMA: anikatriplet1@arizona.edu, MFG-M: mariafernanda.gomezmendez@ucr.edu, KD: katayoon.dehesh@ucr.edu

Running title: Role of stress hormones during singlet oxygen signaling

Word counts
Abstract: 200
Main body:
- Introduction: 1160
- Results: 6436
- Discussion: 1818
- Methods: 1503

Main Figures: 10 color figures
Supplemental information:
- Figures: 13 color figures
- Tables: 27 Tables
- Methods: 4 sections
- Notes: 1 section

Abstract:

In response to environmental stress, chloroplasts generate reactive oxygen species, including singlet oxygen ($^1O_2$), which regulates nuclear gene expression (retrograde signaling), chloroplast turnover, and programmed cell death (PCD). Yet, the central signaling mechanisms and downstream responses remain poorly understood. The *Arabidopsis thaliana plastid ferrochelatase two* (*fc2*) mutant conditionally accumulates $^1O_2$ and involves Plant U-Box 4 (PUB4), a cytoplasmic E3 ubiquitin ligase, in propagating these signals. To gain insights into $^1O_2$ signaling pathways, we compared transcriptomes of *fc2* and *fc2 pub4* mutants. The accumulation of $^1O_2$ in *fc2* plants broadly repressed genes involved in chloroplast function and photosynthesis, while $^1O_2$ induced genes and transcription factors involved in abiotic and biotic stress, the biosynthesis of jasmonic acid (JA), and Salicylic acid (SA). Elevated JA and SA levels were observed in stressed *fc2* plants, but were not responsible for PCD. *pub4* reversed the majority of $^1O_2$-induced gene expression in *fc2* and reduced the JA content, but maintained elevated levels of SA even in the absence of $^1O_2$ stress. Reducing SA levels in *fc2 pub4* restored $^1O_2$ signaling and light sensitivity. Together, this work demonstrates that SA plays a protective role during photo-oxidative stress and that PUB4 mediates $^1O_2$ signaling by modulating its levels.

Keywords: Abiotic stress, *Arabidopsis thaliana*, chloroplast, programmed cell death, reactive oxygen species, singlet oxygen, Jasmonic acid, Salicylic acid

1. Introduction

Plants, as sessile organisms, are constantly exposed to a variety of environmental challenges that can severely influence their growth, development, and ultimately, survival. These challenges (i.e., abiotic, and biotic stresses) trigger multilevel responses that involve stress sensing, signal transduction, regulation of gene expression, and post-translational protein modifications. As sites of photosynthesis, chloroplasts are sensitive to environmental fluctuations, and can act as stress sensors. These organelles produce reactive oxygen species (ROS), including superoxide and hydrogen peroxide at photosystem I (PSI) and singlet oxygen ($^1O_2$) at photosystem II (Triantaphylides and Havaux, 2009). This ROS production is exacerbated under stresses such as excess light (EL) (Triantaphylides et al., 2008), drought (Chan et al., 2016), heat (Sun and Guo, 2016), and salinity (Suo et al., 2017). ROS is highly reactive and can damage cellular macromolecules, including lipids, proteins, and DNA. If unchecked, ROS can impair chloroplast function, disrupt photosynthesis, and lead to cell death. In photosynthetic tissues, $^1O_2$ is the predominant ROS, causing the majority of photo-oxidative damage (Triantaphylides et al., 2008). However, $^1O_2$ can also serve as a stress signaling metabolite, leading to the regulation of nuclear gene expression (via plastid-to-nucleus retrograde signaling), chloroplast degradation, and programmed cell death (PCD) (Dogra and Kim, 2019; D'Alessandro et al., 2020; Woodson, 2022). As $^1O_2$ has a short half-life (~1 μsec) and limited diffusion distance (~200 nm) (Ogilby, 2010), signaling pathways likely employ secondary messengers that exit the chloroplast to elicit a signal. However, the molecular mechanisms by which these signals act are largely unknown.

One challenge to studying $^1O_2$ signaling in plant cells, is that chloroplast $^1O_2$ is produced simultaneously with other types of ROS and cellular damage during natural stresses like EL

(D'Alessandro et al., 2020). Thus, it can be difficult to attribute specific responses to $^1O_2$. Researchers have turned to *Arabidopsis thaliana* mutants that conditionally accumulate chloroplast $^1O_2$ to avoid this complication. One mutant, *plastid ferrochelatase 2* (*fc2*), affects one of two conserved plastid ferrochelatases (FC2) that produces heme from protoporphyrin IX (ProtoIX) in the chloroplast-localized tetrapyrrole (i.e., chlorophylls and hemes) biosynthesis pathway (Chow et al., 1998).

The tetrapyrrole pathway is activated at dawn, leading to an increase in ProtoIX synthesis within chloroplasts (Tanaka et al., 2011). In *fc2* mutants grown under diurnal cycling light conditions, ProtoIX accumulates, becomes photo-sensitized, and quickly produces $^1O_2$ (Kennedy and Pottier, 1992; Woodson et al., 2015). This results in differential regulation of nuclear gene expression, chloroplast degradation, and eventually PCD. Under permissive constant light conditions, *fc2* mutants avoid PCD, but still accumulate a small amount of ProtoIX and $^1O_2$. This leads to the selective degradation of a subset of chloroplasts, which then interact with the central vacuole in a process resembling fission-type microautophagy (Lemke et al., 2021; Fisher et al., 2022; Lemke and Woodson, 2022). Envelope proteins in $^1O_2$-damaged chloroplasts are also ubiquitinated prior to chloroplast degradation and the initiation of PCD (Woodson et al., 2015; Jeran et al., 2021), which may be a mechanism cells use to target damaged chloroplasts for turnover. Such a chloroplast quality control pathway would ensure a healthy population of chloroplasts performing efficient photosynthesis (Zhuang and Jiang, 2019). Additionally, as 80% of leaf nitrogen is stored within chloroplasts, they are prime targets for nutrient redistribution. The induction of PCD may also be a means to avoid necrosis and water loss (D'Alessandro et al., 2020).

Forward genetic screens in *fc2* (Woodson et al., 2015; Lemke and Woodson, 2024) and other $^1O_2$-producing mutants (Wagner et al., 2004) have isolated mutations that block these signals, demonstrating that $^1O_2$-induced cellular degradation is genetically controlled. The cytoplasmic E3 ubiquitin ligase Plant U Box 4 (PUB4) was identified in one such screen as playing a signaling role (Woodson et al., 2015). *fc2-1 pub4-6* mutants (referred as *fc2 pub4* hereafter) showed elevated levels of ProtoIX and $^1O_2$ compared to wt plants, yet the chloroplasts were not ubiquitinated or degraded, nor was PCD initiated. PUB4 has been shown to associate with degrading chloroplasts (Mei et al., 2023), but no PUB4 ubiquitination targets have been identified. Interestingly, PUB4 has also been implicated in multiple cell processes such as asymmetric cell division and cell proliferation of the root meristem (Kinoshita et al., 2015), pattern-triggered immunity (Desaki et al., 2019; Wang et al., 2022; Yu et al., 2022), and cytokinin signaling (Wang et al., 2017). Therefore, PUB4 may be involved in a fundamental process connecting these physiologies.

Although not well understood, the phytohormones Jasmonic acid (JA) and Salicylic acid (SA) can affect chloroplast stress signaling. Synthesis of JA and SA is initiated in the chloroplast, and both regulate the expression of defense-related genes (Reymond and Farmer, 1998; Pieterse et al., 2012). Plants protect themselves against biotrophic and hemibiotrophic pathogens through defense responses induced by SA. At the same time, they safeguard against necrotrophic pathogens and herbivores primarily through defense mechanisms activated by JA and its derivatives (Beyer et al., 2021). SA is required for both local and systemic acquired resistance (SAR) (Zhang et al., 2010) and acts as a signaling molecule in the induction of defense responses against pathogens by regulating the expression of pathogenesis-related (PR) genes such as *PR1* (Kazan and Lyons, 2014).

It is becoming clear that SA and JA also play a role in abiotic stress signaling, particularly in regulating PCD in response to photosynthetic stress (D'Alessandro et al., 2020). EL stress, which can lead to the production of both $^1O_2$ and hydrogen peroxide in chloroplasts, leads to the induction of SA and JA synthesis and signaling (Ramel et al., 2013; Beaugelin et al., 2019). As EL is a complex stress that often includes heat stress, it is not known which ROS may be inducing these responses, although chloroplast $^1O_2$ accumulation in the conditional *flu* mutant has been linked to increased JA and SA levels (Ochsenbein et al., 2006; Przybyla et al., 2008). The impact of these hormones on PCD has been reported, but with conflicting results; different reports suggesting that these hormones can inhibit or induce PCD (Danon et al., 2005; Przybyla et al., 2008).

To understand the molecular mechanisms underlying $^1O_2$ stress signaling and the role of PUB4, here we have taken a whole transcriptome approach to measure the transcriptional responses of *fc2* and *fc2 pub4* plants to cycling light conditions and $^1O_2$ stress. We have previously reported that de-etiolating (greening) *fc2* seedlings exhibit transcriptome changes reflecting photo-oxidative in developing chloroplasts (Woodson, 2015). Here, we extend these findings by demonstrating that $^1O_2$ leads to significant transcriptomic alterations from mature chloroplasts in adult *fc2* plants, particularly affecting chloroplast-associated genes. Interestingly, *pub4* largely reversed the effects of *fc2*, restoring the transcript levels to those observed in wild type plants. Among the processes affected by $^1O_2$, we identified an induction of JA and SA biosynthesis. However, neither is responsible for PCD. Instead, we demonstrate that the *pub4* mutation leads to constitutively high levels of SA, which are necessary to block $^1O_2$–induced PCD. Thus, it is revealed that PUB4 can modulate $^1O_2$ signaling by modulating SA levels, likely through post-translational mechanisms.

2. Results

2.1 The singlet oxygen stress response in adult stage *fc2* mutant is blocked by the *pub4* mutation.

Arabidopsis *fc2* plants, when grown under diurnal light cycling conditions, accumulate singlet oxygen ($^1O_2$), which triggers retrograde signaling, chloroplast degradation, and eventually cell death. This phenomenon is observed in seedlings, where the cotyledons bleach and die (Woodson et al., 2015), and in adult plants, where necrotic lesions appear on the leaves (Lemke and Woodson, 2024). Under constant (24h) light conditions, *fc2* mutants avoid cell death, but selective chloroplast degradation still occurs (Fisher et al., 2022). On the other hand, *fc2 pub4* mutants exhibit elevated levels of $^1O_2$ compared to wt, yet they do not undergo PCD or chloroplast degradation (Woodson et al., 2015; Lemke and Woodson, 2024). The molecular mechanism behind $^1O_2$-induced signaling in *fc2* and its reversal by *pub4* is unknown. To understand this, we scrutinized these mutants in the adult stage under permissive 24h light and $^1O_2$-generating 16h light/8h dark diurnal (cycling) conditions.

In 24h light conditions, four-week-old wt, *fc2*, and *fc2 pub4* plants appear healthy (**Figs. 1a and b**). However, when grown for three weeks in 24h light conditions before transitioning to cycling light conditions for one week, *fc2* begins to exhibit leaf lesions, whereas *fc2 pub4* does not. Trypan blue stains dead cells and was used to quantify cell death (**Figs. 1c-e**). As expected, *fc2* showed a significant increase in cell death compared to wt under two and seven days of cycling light conditions. This was blocked by the *pub4* mutation and *fc2 pub4* showed a level of cell viability similar to wt.

Under 24h light conditions, *fc2* mutants exhibit pale rosettes in comparison to wt, albeit without a significant change in leaf area (**Figs. 1a, b, and f**). On the other hand, *fc2 pub4*

mutants are green, but have significantly reduced leaf area (~30%) compared to wt. Consistently, *fc2* has reduced total chlorophyll content compared to wt, and this effect is reversed by *pub4* (**Fig. 1g**). When transferred to cycling light conditions, *fc2* exhibits impaired growth, with 50% reduced leaf area compared to wt (**Figs. 1a, b, and f**). Conversely, *fc2 pub4* plants do not exhibit any significant growth reduction after a change in light conditions. Taken together, our results show that the *pub4* mutation mitigates the negative impact of chloroplast $^1O_2$ stress in adult stage *fc2* mutants.

2.2 The *pub4* mutation alters the transcriptional responses to singlet oxygen stress

To gain insight into how $^1O_2$ may impact the *fc2* mutant, and what effect the *pub4* mutation has on this response, we performed a whole transcriptome analysis of wt, *fc2*, and *fc2 pub4* plants. Plants were first grown for 16 days in permissive 24h light conditions. To initiate $^1O_2$ stress, they were then shifted to cycling light conditions for two days and leaves were harvested one hour after subjective dawn (cycling sets). A second set of plants remained in 24h light conditions for the full 18 days (24h sets). A Principal Component Analysis (PCA) analysis (**Fig. 1Sa**) and distance matrix plot (**Fig. S1b**) were performed with the replicate samples (three each for a total of 18), indicating that the light condition had the largest effect on global gene expression and that there was less clustering of genotypes under cycling light conditions compared to 24h light conditions. A pairwise comparison of gene expression between the mutants and wt supported this conclusion (**Figs. S2a and b**), with more differences observed in the cycling light conditions irrespective of genotype.

To identify genes controlled by $^1O_2$ and/or PUB4, we performed four pairwise comparisons between wt and the mutants in permissive 24h light or $^1O_2$-inducing cycling light

conditions ("*fc2* vs. wt - 24h", *fc2* compared to wt, grown in 24h light; "*fc2* vs. wt - cycling", *fc2* compared to wt grown in cycling light conditions; "*fc2 pub4* vs. wt - 24h", *fc2 pub4* compared to wt grown under 24h constant light conditions; "*fc2 pub4* vs. wt - cycling", *fc2 pub4* compared to wt grown under cycling light conditions. We then applied a cutoff (Log_2 Fold-Change (FC) > +/- 1.5, *padj* < 0.01) to identify a total of 1682 differentially expressed genes (DEGs) between the datasets (**Fig. 2A** and **Tables S1-5**).

Under 24h light conditions, 69 genes were differentially expressed in "*fc2* vs. wt – 24h", with 60 (87%) showing up-regulation and 9 (13%) showing down-regulation (**Fig. 2B**). Among the up-regulated genes, there was an enrichment of gene ontology (GO) terms associated with abiotic stress (e.g., heat, response to ROS) (**Fig. S3a** and **Table S6**), but no GO-terms were enriched among down-regulated genes. Under cycling light conditions, the response in "*fc2* vs. wt – cycling" was pronounced with 1532 genes exhibiting differential expression compared to wt. Among these, 1230 (80%) were upregulated and 302 (20%) were down-regulated (**Fig. 2c**). The up-regulated genes were enriched for GO terms broadly related to stress, predominantly biotic stress-related (**Fig. 3a** and **Table S7**), including "response to jasmonic acid", "response to salicylic acid", "response to wounding", and "response to bacterium". In addition, terms related to abiotic stress such as "response to hypoxia" and "response to oxidative stress" were enriched. Conversely, the down-regulated genes were enriched for GO-terms related to photosynthesis and growth including "photosynthesis light harvesting in PSII and PSI" and "regulation of growth" **(Fig. 3b** and **Table S7**). As there are no $^1O_2$-associated GO-terms, we compared DEGs to the list of the core $^1O_2$ response genes (24 up-regulated and 11 down-regulated) identified by a meta-analysis (Tano et al., 2023). In *fc2* under cycling light conditions, 18 of the 24 up-regulated and 2 of the 11 down-regulated passed the cutoff values (compared to wt), while heatmaps show that

all 35 genes followed the expected expression patterns (**Figs. 3c and d**). This expression depended on $^1O_2$ accumulation, as none of these genes were differentially expressed under 24h light conditions, compared to wt.

Next, we assessed the effect the *pub4* mutation has on these responses. Under 24h light conditions, 71 DEGs were identified in "*fc2 pub4* vs. wt - 24h" (46 (65%) upregulated and 25 (35%) downregulated) (**Fig. 2b**). However, only a small subset of these DEGs were shared with "*fc2* vs. wt – 24h", indicating that the majority of the upregulated (82%) and downregulated (89%) DEGs in *fc2* are reversed by the *pub4* mutation in 24h light conditions (**Table S8**). However, the up-regulated genes shared by "*fc2* vs. wt – 24h" and "*fc2 pub4* vs. wt – 24h" were enriched for abiotic stress-related GO-terms, including "response to salt", "response to ROS," and "response to heat" (**Fig. S3b** and **Table S9**). Furthermore, the upregulated DEGs specific to "*fc2 pub4* vs. wt – 24h" were enriched for the "defense response" GO term (**Table S9**) suggesting that the *pub4* mutation does not entirely reverse the stress phenotype of *fc2* and may lead to a degree of constitutive stress response in the absence of $^1O_2$.

In cycling light conditions, 191 DEGs were identified in "*fc2 pub4* vs. wt – cycling" with 142 (74%) showing up-regulation and 49 (26%) showing down-regulation (**Fig. 2c**). As in 24h light conditions, the majority of upregulated (93%) and downregulated (94%) DEGs found in "*fc2* vs. wt – cycling" were not shared with "*fc2 pub4* vs. wt – cycling", (**Table S8**) suggesting that *pub4* reverses the majority of gene expression in *fc2* during cycling light conditions. This was consistent for the core $^1O_2$ response genes, none of which were differentially expressed in "*fc2 pub4* vs. wt – cycling" (**Figs. 3c and d**).

However, among the up-regulated DEGs shared by "*fc2* vs. wt – cycling" and "*fc2 pub4* vs. wt – cycling", many GO-terms associated with biotic and abiotic stress remained enriched

(**Fig. S3c** and **Table S10**). However, notably absent were terms associated with jasmonic and salicylic acid signaling. Only GO-terms associated with wax and fatty acid biosynthesis were enriched among shared down-regulated genes, while terms associated with photosynthesis were entirely absent (**Figs. S3d** and **Table S10**). As *pub4* does not fully reverse the stress response of *fc2* under cycling light conditions, it may partially alleviate the negative impact on photosynthesis. We validated these RNA-seq data by confirming the relative expression changes of nine DEGs identified in "*fc2* vs. wt – cycling" and "*fc2 pub4* vs. wt – cycling" using RT-qPCR (**Fig. S3e**).

2.3 WRKY and NAC transcription factor targets are induced by singlet oxygen and activation of NAC targets is blocked by the *pub4* mutation

Given the significant effect $^1O_2$ has on gene expression in *fc2*, we next asked if any transcriptional regulatory mechanisms are involved. To this end, we identified additional DEGs in each of the four pairwise comparisons by relaxing our cutoff criteria ($\log_2$FC > +/- 1 and *padj* < 0.01) (**Table S11**) and compared the resulting DEG list to a curated list of transcription factors (TFs) (**Table S12**) (Jin et al., 2014; Jin et al., 2017). This led to the identification of 254 differentially expressed TFs (DETFs) in our data set (**Fig. S4a** and **Table S12**). 219 DETFs were identified in "*fc2* vs. wt – cycling", with 216 of these DETFs possibly dependent on $^1O_2$, as they were not found in "*fc2* vs. wt – 24h" (**Fig. S4b**). We only identified 41 DETFs in "*fc2 pub4* vs. wt – cycling", and only 18 of these DETFs were shared with "*fc2* vs. wt – cycling", suggesting that most of what is observed in *fc2* can be reversed by the *pub4* mutation (**Fig. S4c**). We also analyzed these DETFs for enrichment of specific families of TFs (**Fig. S4d** and **Tables S13** and **14**). WRKY, Ethylene Response Factor (ERF), and NAC TF family member genes were

significantly enriched in "*fc2* vs. wt – cycling", while only WRKYs and ERFs were significantly enriched (albeit in reduced numbers) in "*fc2 pub4* vs. wt – cycling." For down-regulated TFs, CONSTANS (CO)-like, basic/helix-loop-helix (bHLH), and myeloblastosis (MYB)-related TFs were enriched in "*fc2* vs. wt – cycling", and MIKC MADS TFs were enriched in "*fc2 pub4* vs. wt – cycling." Together these data suggest $^1O_2$ accumulation leads to the reprogramming of hundreds of TF's. This mostly involves PUB4, although some ERFs and WRKYs may be regulated independently.

Next, we performed a GO term enrichment analysis to identify processes that may be affected by these DETFs (**Table S15**). DETFs identified in "*fc2* vs. wt – cycling" were enriched for GO-terms associated with stress hormone signaling (SA, JA, ABA, and ethylene), biotic defense response (e.g., response to bacterium and chitin), response to abiotic stresses (e.g., hypoxia and water deprivation), and regulation of leaf senescence (**Fig. S5a**). Among down-regulated DETFs, only the GO-term "gibberellic acid signaling" was enriched. In contrast, only ethylene signaling GO-terms were observed to be enriched in up-regulated DETFs within "*fc2 pub4* vs. wt – cycling" (**Fig. S5b**). Of the WRKY TFs upregulated in "*fc2* vs. wt – cycling", we observed stress hormone signaling (SA and JA), biotic defense response (response to bacterium and chitin), response to abiotic stresses (water deprivation), and regulation of leaf senescence. Among ERF TFs, we observed enrichment of ethylene stress hormone signaling, response to abiotic stresses (water deprivation) terms. For NAC TFs, we observed enrichment of the regulation of leaf senescence represented (**Fig. S5c**). In "*fc2 pub4* vs. wt – cycling", on the other hand, we only observed SA stress hormone signaling and ethylene stress hormone signaling to be associated with the WRKY and ERF TFs, respectively (**Fig. S5d**). These observations suggest

that the *pub4* mutation mediates the chloroplast $^1O_2$-induced activation of TFs involved in JA signaling, defense responses, and leaf senescence, but does not affect SA signaling.

Next, we performed a transcription factor enrichment analysis (TFEA) to investigate if these induced TFs are responsible for the observed transcriptional response. We observed targets of 179 and 115 TFs in the "*fc2* vs. wt – cycling" comparison to be represented in upregulated and down-regulated DEGs, respectively (**Figs. S6a and b, Table S16**). The *pub4* mutation mostly reversed this trend with only 39 and 7 TFs shared among the up-regulated and down-regulated DEG targets, respectively, in "*fc2 pub4* vs. wt – cycling". Among the TFs identified, WRKYs, NACs, bZIP, MYB, and BES1 TF targets were enriched in "*fc2* vs. wt – cycling" (**Fig S6c** and **Table S107**). Notably, ERF TF targets were not enriched in this analysis, even though ERF TFs were enriched in the DETF analysis. *pub4* appeared to reverse these effects, except for WRKYs, 30 of which were enriched in "*fc2 pub4* vs. wt – cycling". Interestingly, these 30 WRKY TFs are all shared with "*fc2* vs. wt – cycling", suggesting *pub4* has little impact on their function.

When we compared the lists of TFs from the DETF analysis and TFEA, we found an overlap of 57 and 5 TFs, respectively between "*fc2* vs. wt – cycling" and "*fc2 pub4* vs. wt cycling" (**Figs. S6d and e** and **Table S18**). This maintained the general trend of enrichment of WRKYs (23) and NACs (16) in "*fc2* vs wt – cycling", and the retention of WRKYs (5) in *"fc2 pub4* vs. wt – cycling". Interestingly, the five WRKYs present in "*fc2 pub4* vs. wt – cycling" include WRKY33 and WRKY40, which respond to $^1O_2$ (Lai et al., 2011; Dogra et al., 2017; Li et al., 2023) and SA signaling (Dong et al., 2003). Together, these results suggest that $^1O_2$ induces a robust transcriptional change by regulating the expression of hundreds of TFs, particularly WRKY and NAC family members. The *pub4* mutation may block this response, in part, by

affecting the expression (WRKYs and NACs) and activation (WRKYs) of some of these TFs, while still retaining part of the WRKY-directed stress response.

2.4 Singlet oxygen affects plastid protein gene expression and regulation

Under cycling light conditions, downregulated DEGs in *fc2* were predominantly associated with chloroplasts, particularly the photosynthetic light reactions (**Fig. 3b**). To further understand how $^1O_2$ affects chloroplasts and photosynthesis at the level of transcript accumulation, we used the list of 2495 plastid protein-encoding genes (PPEGs) (both plastid- and nuclear-encoded) from the Plant Proteome database (PPDB) (http://ppdb.tc.cornell.edu/dbsearch/subproteome.aspx). After removing splice variants and genes with unavailable data, a list of 1730 unique PPEGs was established and their relative expression within the RNA-seq data set were assessed (**Fig. 4a** and **Table S19**). Under cycling light conditions, 1,135 PPEGs (65%) exhibited significant alterations in "*fc2* vs. to wt – cycling" (*padj* < 0.01) (975 (56%) downregulated and 160 (9%) upregulated) (**Fig. 4b**). This effect was partially reversed by *pub4* with only 26% of PPEGs (5% up-regulated and 21% down-regulated) exhibiting altered expression in "*fc2 pub4* vs. wt – cycling."

To gain a deeper insight as to which chloroplast compartments were being affected by $^1O_2$ in *fc2* under cycling light conditions, the PPEGs were further sub-categorized by predicted protein localization (envelope, thylakoid, plastoglobule, and stroma (plus other localizations)) (**Fig. 4c**). While genes in all four categories were both up- and down-regulated in *fc2*, genes encoding proteins in the thylakoid membrane appeared to be disproportionally down-regulated. To quantify this distribution, we further divided proteins into predicted chloroplast sub-compartments (including nucleoid, ribosome, and unspecified) and applied a significance cutoff

of *padj* < 0.01 (**Fig. 4d**). As expected, the thylakoid membrane compartment is the most negatively affected in *fc2*, along with the ribosome, and nucleoid compartments. This implies that $^1O_2$ stress in chloroplasts predominantly influences transcripts encoding photosynthetic and gene expression machinery.

To determine the functions of these genes, we next performed GO-term analyses of PPEGs affected in "*fc2* vs. wt - cycling" (**Table S20**). The 160 up-regulated PPEGs were enriched for GO-terms associated with chorismate biosynthesis (a critical step in SA biosynthesis), senescence (chlorophyll catabolism), and amino acid synthesis (phenylalanine and tryptophan) (**Fig. S7a**). Among the 975 down-regulated PPEGs, GO-terms associated with photosynthesis (light and carbon reactions) and ribosome assembly (rRNA processing) were enriched (**Fig. S7b**). A comparison with differentially expressed PPEGs in "*fc2 pub4* vs. wt – cycling" showed that the *pub4* mutation reversed most of the changes of gene expression in *fc2* (**Fig. 4e**). However, both mutants were still enriched for GO-terms associated with stress (high light, cold, and heat) and photosynthesis (light and carbon reactions) among up- and down-regulated DEGs, respectively (**Fig. S7c and d**). Thus, the *pub4* mutation reverses expression of genes involved in stress responses (induction of SA biosynthesis, chlorophyll catabolism) and lessens the negative impact on photosynthesis.

Some differentially expressed PPEGs were unique to "*fc2 pub4* vs. wt – cycling." Among the 60 up-regulated PPEGs, there was enrichment for GO-terms related to plastid gene expression (transcription, translation, rRNA processing), nucleotide import, and protein import (**Fig. S7e**). Conversely, the 39 down-regulated PPEGs were enriched for GO terms related to SA biosynthesis (i.e., chorismate biosynthesis) and aromatic amino acid synthesis (**Fig. S7f**). These latter terms were associated with the upregulated PPEGS in "*fc2* vs. wt – cycling." These results

suggest that the *pub4* mutation leads to an increases plastid gene expression and chloroplast development while down-regulating SA biosynthesis pathways.

To test if PPEGs in the nucleus or plastid are more affected by $^1O_2$ stress conditions, we compared expression patterns of plastid (40 genes) and nuclear-encoded genes (51) encoding components of the photosynthetic light reactions (as well as RBCL in the plastid) **(Figs. S8a and b)**. Of the plastid genes, three genes encoding ATP synthase subunits were differentially expressed in "*fc2* vs. wt – cycling" (*padj* < 0.01). In contrast, all 51 nuclear genes were repressed in "*fc2* vs wt - cycling." For each of these genes, the *pub4* mutation reduced the strength of the repression, but 44 were still significantly repressed in "*fc2 pub4* vs. wt - cycling."

Next, we tested if plastid-encoded gene expression correlated with protein abundance. Immunoblotting was used to compare the accumulation pattern of the plastid-encoded proteins RbcL (large subunit of RuBisCO), PsaA (PSI complex subunit), PsbD/D2 (PSII complex subunit), and PetB (cytochrome b_6f complex subunit). Despite a mild effect on plastid-encoded transcripts, both RbcL and PsaA were less abundant in *fc2* plants in cycling light, compared to 24h light conditions (**Figs. 4f and g**). PetB accumulation, on the other hand, was not significantly altered (**Figs. 8f**). Surprisingly, the D2 protein was more abundant in cycling light-stressed plants (**Fig. 4h**). These effects were slightly reversed by *pub4*, although the D2 protein still accumulated to higher levels in *fc2 pub4* plants grown under cycling light conditions. We also tested protein accumulation in plants after seven days in cycling light conditions and observed similar patterns of protein accumulation (**Figs. S8c-e, g**). Together, this suggests that $^1O_2$ affects nuclear and plastid-encoded transcripts differently, and may also affect plastid-encoding protein levels through post-translational regulatory mechanisms.

2.5 Senescence is induced in singlet oxygen-stressed *fc2* plants.

When *fc2* mutants are subjected to cycling light conditions, senescence-like phenotypes are induced. Characterized by pale leaves, an increase in plastoglobules, degradation of chloroplasts, and cell death, these phenotypes are reversed by the *pub4* mutation (Woodson et al., 2015; Lemke et al., 2021; Fisher et al., 2022). We also observed an enrichment of senescence-related GO-terms in genes up-regulated in "*fc2* vs. wt - cycling" (but not in "*fc2 pub4* vs. wt - cycling") (**Tables S7** and **S10**). To investigate if canonical senescence pathways play a role in $^1O_2$ stress, we measured the expression of genes involved in regulating leaf senescence within the RNA-Seq data set. We compared expression patterns of 128 genes, associated with the GO-term "leaf senescence" (GO: 0010150) (**Fig. S9a** and **Table S21**). Only 2% were up-regulated in "*fc2* vs. wt - 24h", but 47% were up-regulated in "*fc2* vs. wt – cycling" (*padj* < 0.01). This effect in cycling light conditions was largely reversed by the *pub4* mutation with only 11% of genes being induced in "*fc2 pub4* vs. to wt – cycling."

To refine our analysis, we selected 38 senescence-associated and regulatory genes from the literature (**Fig. 5a** and **Table S21**) (Bresson et al., 2018; Kim et al., 2018). In 24h light conditions, none of these genes were differentially expressed in "*fc2* vs. wt – 24h" (*padj* < 0.01). However, under cycling light conditions, most of these genes were induced (24) or repressed (4) in "*fc2* vs. wt - cycling." Two of the repressed genes, *CAB1* and *RBCS1A*, are also repressed during senescence (Bresson et al., 2018). These patterns were mostly reversed by the *pub4* mutation (5 and 1 were induced or repressed, respectively, in "*fc2 pub4* vs. wt – cycling"). Notably, four of the five *SENESCENCE-ASSOCIATED GENES* (*SAGs*) tested were induced in "*fc2* vs. wt – cycling." The significant up-regulation of genes encoding the transcription factors (and positive regulators of senescence (Zentgraf et al., 2010; Christiansen and Gregersen, 2014)

ANAC016, *ANAC019*, *ANAC72*, and *WRKY53* in "*fc2* vs. wt – cycling," suggests that they may be initial targets of the $^1O_2$ signal. Additionally, *POLYAMINE OXIDASE 1* (*PAO1)*, encoding an enzyme involved in chlorophyll catabolism, was induced. Together, these data suggest that senescence pathways are induced in *fc2* mutants under $^1O_2$ accumulating conditions, which was reversed by *pub4*.

To test this assertion, detached leaves from plants grown in 24h light conditions were floated on water and incubated in the dark for three days to induce early senescence (Qi et al., 2015). All three genotypes exhibited some level of senescence as evidenced by the visual yellowing of leaves (**Fig. 5b**). This senescence remained constant in the three genotypes and did not significantly change if plants were initially gown under cycling light conditions (**Fig. S9b**). Next, we measured the maximum photosynthetic efficiency of PSII (F_v/F_m) values of these leaves. Without dark incubation, F_v/F_m values were similar in all genotypes (**Fig. S9c**). After dark incubation, the values decreased, but to different levels. F_v/F_m values were highest for wt (mean = 0.77) and lowest for *fc2* mutants (mean = 0.61), while *fc2 pub4* was in between (mean = 0.7) (**Fig. 5c**). The chlorophyll content was highest in wt leaves and significantly lower in both *fc2* and *fc2 pub4* mutants (**Fig. 5d**). A similar pattern was observed in cycling light conditions (**Figs. S9d and e**).

Next, we added 100 µM methyl jasmonate (MeJA) before dark incubation to enhance senescence (Qi et al., 2015). Under these conditions, both wt and *fc2* leaves showed pronounced yellowing, whereas *fc2 pub4* leaves showed less visual senescence (**Fig. 5b**). In this case, both F_v/F_m values and total chlorophyll content were significantly lower in *fc2* compared to wt (**Figs. 5c and d**). In the case of *fc2 pub4*, F_v/F_m values resembled those of wt, while total chlorophyll content was closer to *fc2*. Similar results were obtained with plants initially grown under cycling

light conditions (**Figs. S9d and e**). Together, these results suggest that *pub4* alleviates senescence pathways whether they are activated by $^1O_2$ or JA treatments.

2.6 Singlet oxygen stress leads to the induction of jasmonic acid synthesis and signaling.

$^1O_2$-stressed *fc2* mutants showed an enrichment of genes associated with jasmonic acid (JA) synthesis and metabolism (**Fig. 3a**), suggesting that JA synthesis may be induced by $^1O_2$ accumulation. This is in line with the up-regulation of senescence-related transcripts (**Figs. 5a and S9a**) (Hu et al., 2017). To test this, we used the RNA-seq data set to analyze the expression of 11 key genes involved in JA biosynthesis and signaling (**Fig. 6a** and **Table S22)**. Eight of these genes (including seven involved in biosynthesis) were significantly upregulated in "*fc2* vs. wt – cycling," and only *DAD1* was still induced in "*fc2 pub4* vs. wt – cycling" (*padj* < 0.01). To test if this change in gene expression leads to altered JA levels, plants were assessed for JA content (**Fig. 6b**). Under 24h conditions, all genotypes accumulated similar levels of JA. After being shifted to cycling light conditions for two days, *fc2* plants accumulated ~6-fold more JA than wt. The *pub4* mutation reversed this phenomenon.

Next, we used the RNA-seq data set to analyze expression of 58 genes associated with the GO term "JA mediated signaling pathway" (GO:0009867) ((**Fig. 6c** and **Table. S22**). Only one gene was differentially expressed (*padj* < 0.01) in "*fc2* vs. wt – 24h." However, under cycling light conditions, 37 genes were differentially expressed (23 up and 14 down) in "*fc2* vs. wt - cycling." This included *MYC2,* a "master switch" of JA signaling (Kazan and Manners, 2013; Breeze, 2019). Furthermore, the *pub4* mutation reverses most of this response, with 8 of these selected JA genes in "*fc2 pub4* vs. wt – cycling" being differentially expressed. Thus, the upregulation of biosynthesis genes, elevated levels of JA content, and differential expression of

signaling genes indicate that JA signaling is triggered in response to $^1O_2$ stress in *fc2* mutants and blocked by the *pub4* mutation.

2.7 Blocking jasmonic acid synthesis does not suppress cell death in fc2 plants.

Due to reported links between JA and $^1O_2$ signals (Ramel et al., 2013), we hypothesized that JA accumulation in *fc2* mutants could be responsible for $^1O_2$-induced PCD. To this end, we introduced an *aos* loss-of-function mutation into the *fc2* background to test if reducing JA levels can reduce PCD. AOS is a key enzyme involved in the biosynthesis of JA (**Fig. 6a**) and a knock-out mutations block JA biosynthesis (Park et al., 2002).

We first tested the ability of the *aos* mutation to suppress PCD in *fc2* seedlings, which were germinated in 24h light or $^1O_2$-generating 6h light/18h dark diurnal (short-day) light conditions. In 24h light conditions, all genotypes appeared healthy (**Fig. S10a**), and no cell death could be detected by trypan blue staining (**Figs. 7a and S10b**). In short-day conditions, *fc2* seedlings bleached and cell death could be detected in cotyledons (**Figs. 7a and b and S10a**). As expected, the *pub4* mutation completely blocked this cell death. The *aos* mutation, however, only had a mild effect. *fc2 aos* seedlings still suffered significantly more cell death than wt, but it was reduced compared to *fc2*. Four independently resolved lines of *fc2 aos* were tested, and all had similar phenotypes in these conditions. This suggests that $^1O_2$-indued PCD is still at least partly active in these mutants despite JA synthesis being blocked.

Next, we assessed adult phenotypes in 4-week-old plants. All genotypes appeared healthy when grown under 24h light conditions (**Fig. 7c**) and the *aos* mutation did not significantly affect chlorophyll content (**Fig. S10c**). *fc2* and *fc2 aos* plants also had similar leaf areas (**Fig. 7d**) and biomass (**Figs. 7e and f**), suggesting that the *aos* mutation did not severely affect growth.

If plants are shifted to cycling light conditions for the fourth week, *fc2* mutants develop necrotic lesions (**Fig. 7c**), exhibit reduced leaf area (**Fig. 7g**) and reduced biomass (**Figs. 7h and i**). While the *pub4* mutation blocks lesion formation, the *aos* mutation does not (**Fig. 7c**). Furthermore, the *fc2 aos* mutant does not have significantly reduced leaf area and dry weight biomass compared to *fc2* (**Figs. 7h and i**). This suggests that high JA content in *fc2* is not directly responsible for PCD under $^1O_2$-producing conditions.

2.8 Singlet oxygen stress in the *fc2* mutant leads to the induction of Salicylic acid synthesis and signaling.

The GO-terms "response to SA" and "chorismate biosynthesis" were strongly enriched among genes and TFs upregulated in *fc2* in response to $^1O_2$ stress (**Figs. 3a, S5a and c**, **S7a** and **Table S7**) leading us to hypothesize that SA levels and/or signaling may also be induced. To this end, we assessed the relative expression of ten genes associated with SA synthesis (**Figs. 8a and b** and **Table S23**) (Dempsey et al., 2011). In "*fc2* vs. wt – 24h," none of these genes were significantly induced (*padj* < 0.01). Under cycling light conditions, however, four of these genes were significantly induced in "*fc2* vs. wt - cycling." This included *ISOCHORISMATE SYNTHASE1* (*ICS1*) and *PBS3*, but none of the genes encoding phenylalanine ammonia-lyase (*PAL1-4*). Thus, it appears the dominant ICS pathway, rather than the PAL pathway (**Fig. 8a**), is induced in *fc2* under cycling light conditions. This response was mostly reversed by the *pub4* mutation. Some of the ICS pathway genes were mildly upregulated in "*fc2 pub4* vs. wt – 24h/cycling" but these differences were not statistically significant.

We also measured the expression of 22 genes associated with the regulation of SA biosynthesis (Huang et al., 2020) and observed a similar pattern (**Fig. 8c** and **Table S23**). In

constant light conditions, the expression of only one gene was significantly altered in "*fc2* vs. wt – 24h" (*padj* < 0.01). However, under cycling light conditions, 17 genes (77%) were significantly affected (15 up-regulated and 2 down-regulated) in "*fc2* vs. wt - cycling." This effect was mostly reversed by *pub4*, but 6 (WRKYs 8, 28, 20, and 49) and 2 (WRKYs 28 and 46) of these genes were misregulated in "*fc2 pub4* vs. wt – cycling" and "*fc2 pub4* vs. wt – 24h," respectively.

Next, we measured SA levels in 17-day-old plants to determine if these changes in transcript levels led to increased hormone levels. Under constant light conditions, there was no significant difference in SA content between *fc2* and wt (**Fig. 8d**). However, upon exposure to cycling light conditions for two days, *fc2* accumulated ~40-fold more SA content than wt. Unlike JA, the *pub4* mutation only reduced this induction by 50%. Surprisingly, SA content increased more than 20 times in *fc2 pub4* under constant light conditions. This suggests that SA content is constitutively high in *fc2 pub4* plants despite only a mild effect on some genes involved in SA synthesis (**Fig. 8b**) and regulation (**Fig. 8c**)). To test if the high level of SA in *fc2 pub4* plants was leading to a canonical SA response, we identified DEGs between *fc2* and *fc2 pub4* in constant light conditions (*padj* < 0.01) and compared them to 204 SA-responsive genes (**Table S24)** (Zhou et al., 2015b). 48 (24%) of these genes were differentially expressed between *fc2* and *fc2 pub4* (42 (88%) and 6 (12%) upregulated and downregulated, respectively). Thus, the high level of SA in *fc2 pub4* is activating a mild transcriptional SA response.

2.9 Lowering Salicylic acid content in *fc2* mutants impairs light stress tolerance.

We observed that *fc2* mutants conditionally accumulated SA under cycling light conditions, correlating with the PCD phenotypes (**Fig. 8d**). Elevated SA levels have been

observed in lesion-mimic mutants, and can trigger the hypersensitive response and cell death (Radojičić et al., 2018). Thus, the high level of SA in *fc2* mutants may be responsible for $^1O_2$-induced PCD. However, we also observed constitutively high SA levels in *fc2 pub4* regardless of the light condition. Therefore, an alternative hypothesis is that SA can protect *fc2* mutants from $^1O_2$-induced PCD.

To distinguish between these two possibilities, we used the *eds16*/*ics1* mutation to decrease SA synthesis in our mutant lines (Wildermuth et al., 2001). *EDS16*/*ISC1* encodes isochorismate synthase that converts chorismic acid to isochorismic acid (**Fig. 8a**). In the *fc2* background, this mutation blocked the accumulation of SA under cycling light conditions and *fc2 eds16* mutants had similar levels of SA to wt (**Fig. 9a**). Interestingly, the *fc2 eds16* mutant did accumulate more JA than *fc2* under cycling light conditions (**Fig. 9b**). This was likely dependent on $^1O_2$, as *eds16* single mutants did not accumulate high levels of JA.

First, we tested if lowered SA biosynthesis in *fc2* seedlings can reduce $^1O_2$-induced PCD. All genotypes appeared healthy after seven days under 24h light conditions (**Fig. S11a**). Under short-day conditions, however, *fc2* mutants exhibit a PCD phenotype. The *fc2 eds16* seedlings appeared similar to *fc2*, suggesting that the *eds16* mutation did not suppress cell death. Eight independently resolved lines of *fc2 esd16* were tested, and all had similar phenotypes in these conditions.

Next, we assessed the phenotypes of 4-week-old plants. In constant light conditions, all genotypes, including *fc2 eds16*, appeared healthy (**Fig. 9c**) and did not exhibit leaf lesions (**Figs. 9d and S11b**). The *eds16* mutation did not significantly affect total chlorophyll content (**Fig. S11c**) *fc2 eds16* mutants did have reduced fresh weight and dry weight biomass compared to *fc2*

(**Figs. 9e and f**) indicating some level of growth impairment. This was specific to the *fc2* background, as *eds16* single mutants were similar to wt plants.

As expected, *fc2* mutants exhibited leaf lesions within one week of cycling light conditions (**Figs. 9c, d, and g**). However, the *eds16* mutation did not affect this lesion formation, and *fc2 eds16* mutants exhibited similar levels of PCD as *fc2*. Furthermore, we observed that *fc2 eds16* adult plants developed necrotic lesions when moved from the lab bench back to growing conditions, suggesting that they were sensitive to large fluctuations in light intensity. To test this, a light shift (LS) experiment was designed where plants were grown in constant light conditions (120 µmol m^{-2} sec^{-1}) for 3 weeks, shifted to dim light (~4 µmol m^{-2} sec^{-1}) for 8 hours, and then returned to constant light conditions for five days (**Fig. 9h**). Under these conditions, wt plants were healthy, but *fc2* mutants accumulated leaf lesions, suggesting that these plants are sensitive to shifts in light intensity (**Figs. 9c, d, and i**). Lesions were absent in *fc2 pub4* mutants suggesting that the lesions in *fc2* were induced by $^1O_2$ stress. The *eds16* mutation, however, did not reduce lesion formation and *fc2 eds16* mutants exhibited elevated PCD compared to *fc2*. Under light shift conditions, *fc2 eds16* also showed significantly reduced fresh weight and dry biomass than *fc2*, possibly due to increased water loss and decreased growth, respectively (**Figs. 9j and k**). Again, these effects of *eds16* were specific to the *fc2* background as the *eds16* single mutant was similar to wt. Together, these data demonstrate that higher SA content in *fc2* is likely not responsible for PCD under cycling light conditions, and may even offer some protection to *fc2*.

2.10 The elevated levels of Salicylic acid in *fc2 pub4* mutants are partly responsible for the reduction of cell death in cycling light conditions

The above results suggest that SA is not responsible for PCD in *fc2* mutants under cycling light conditions, and instead, may be important for tolerance. As such, we next tested if the constitutively high levels of SA in *fc2 pub4* are responsible for this mutant's ability to avoid $^1O_2$-induced PCD. To test this, we introduced the *eds16* mutation into *fc2 pub4*, which reduced SA content in *fc2 pub4 eds16* to wt levels (**Fig. 9a**). As seven-day-old seedlings grown under 24h light conditions, *fc2 pub4 eds16* and all tested genotypes lacked lesions (**Figs. 10a and S11d**). Under short day light conditions, *fc2* seedlings exhibited PCD, which was reversed in *fc2 pub4* (**Figs. 10a and b**). In line with the high levels of SA blocking PCD, *fc2 pub4 eds16* seedlings exhibited restored cell death. Four independently resolved lines of *fc2 pub4 esd16* were tested, and all had similar phenotypes in these conditions.

Next, we tested these genotypes in the adult phase. Under 24h light conditions, four-week-old *fc2 pub4 eds16* plants appeared healthy with no visible lesions (**Figs. 10c and S11e**). The fresh weight and dry biomass in *fc2 pub4 eds16* were significantly higher than *fc2 pub4* (**Fig. 10d and e**) and the total chlorophyll content in *fc2 pub4 eds16* was decreased compared to *fc2 pub4* (**Fig. 10f**). These effects were specific to *fc2 pub4* as *eds16* did not have these effects in the wt or *fc2* backgrounds (*i.e.*, *eds16* and *fc2 eds16*).

To test the effect of *eds16* during $^1O_2$ stress, plants were subjected to cycling light conditions or a light shift for seven and five days, respectively. As expected, *fc2* mutants exhibited leaf lesions, which were blocked in *fc2 pub4* mutants (**Figs. 10g and h and S11f and g**). Similar to the seedling stage, *fc2 pub4 eds16* mutants exhibited restored lesion formation and were similar to *fc2* and *fc2 eds16*. This effect was specific to *fc2 pub4*, as *eds16* in the wt or *fc2* backgrounds did not significantly affect lesion formation. Together, these data show that several

fc2 pub4 phenotypes (blocked PCD, increased chlorophyll content, and reduced biomass) depend on this mutant's high levels of SA.

We next tested if *eds16* could also reverse the EL tolerance of *fc2 pub4* (Tano et al., 2023; Lemke and Woodson, 2024). To this end, we exposed 21-day-old plants grown in 24h light conditions to 24h of EL (1,500 µmol photons sec^{-1} m^{-2}) at 10°C. As expected, wt and *fc2* plants developed leaf lesions (**Figs. 10i and j**). The *pub4* mutation attenuated this lesion formation and *pub4* and *fc2 pub4* mutants accumulated fewer lesions than wt and *fc2*, respectively. In line with the above results, the *eds16* mutation restored EL sensitivity to *fc2 pub4*; *fc2 pub4 eds16* mutants accumulated significantly more lesions than *fc2 pub4*. The effect of *eds16* appeared specific to the *fc2 pub4* background as *eds16* and *fc2 eds16* had similar lesions to wt and *fc2*, respectively.

The above results suggest that high SA content is necessary for *fc2 pub4* plants to reduce photo-oxidative damage and $^1O_2$ signaling. To test if high SA content alone is sufficient, we sprayed three-week-old plants with 4 mM SA before subjecting them to cycling light conditions for two days. The SA treatment had no significant effect on lesion formation and *fc2* plants still experienced a similar level of PCD in leaves as untreated *fc2* plants (**Figs. S12a-b**). The analysis of four SA-responsive transcripts by RT-qPCR (*PR1*, *WRKY33*, *WRKY40*, and *PAD4*) in these plants confirmed that the SA response was being induced (**Fig. S12c-f**). Interestingly, all four transcripts were also induced in *fc2 pub4* plants, relative to *fc2*, before SA treatment, supporting the conclusion that *fc2 pub4* plants have a constitute SA response. Together, these results show that the high SA content in *fc2 pub4* is necessary to protect against $^1O_2$, but is not sufficient.

2.11 $^1O_2$ stress affects the expression of anthocyanin biosynthesis and regulator genes

During our experiments, we observed that *fc2 pub4* mutants can turn dark colors (**Fig. 1a**) indicating that they may be accumulating anthocyanins that could protect them from light stress. When grown in 24h light conditions or shifted to cycling light conditions, no significant difference in anthocyanin content was observed between wt and *fc2* after two or seven days (**Figs. S13 a and b**). However, *fc2 pub4* had a ~2-fold higher anthocyanin content than *fc2*, irrespective of the light condition or time point. An analysis of genes involved in anthocyanin biosynthesis and regulation (**Table S25**) suggested that the *fc2 pub4* mutant mildly upregulates the majority of these genes compared to wt, which may be responsible for the high anthocyanin content in this mutant (**Fig. S14c** and **Supplementary Notes 1**).

To determine if the high SA content in *fc2 pub4* is responsible for the elevated anthocyanin content, we measured anthocyanin content in *fc2 eds16* and *fc2 pub4 eds16* mutants (**Fig. S14d**). The *fc2 pub4 eds16* mutant still had elevated anthocyanin content (despite being sensitive to cycling light conditions (**Fig. 10h**)), and *fc2 eds16* mutants had elevated anthocyanin compared to *fc2*, even though they are less tolerant to cycling light conditions (**Fig. 10h**)). Together, these results suggest that *fc2 pub4* mutants do accumulate high levels of anthocyanins, but this phenotype is not correlated to a reduction of light-induced PCD. Thus, SA likely leads to photoprotection by another mechanism.

3. Discussion

Singlet oxygen specifically impacts chloroplast function

A large body of evidence has demonstrated that chloroplast $^1O_2$ can trigger multiple cellular signals affecting chloroplast degradation, retrograde signaling, and PCD (Dogra and Kim, 2019; D'Alessandro et al., 2020; Woodson, 2022), but these signals are poorly understood.

Here, we show that $^1O_2$ accumulation in *fc2* leads to a relatively large change in the transcriptome (1,532 DEGs) (**Figs. 2a and c**). Although these genes are involved in many aspects of cell physiology, there was a clear connection to chloroplast function and photosynthesis as the repressed genes (302 DEGs) were strongly enriched for processes involving photosynthesis (**Fig. 3b**). A separate analysis of PPEGs demonstrated that $^1O_2$ significantly affected the expression of more than half of plastid protein-encoded transcripts (1,135 of 1,730), with most being repressed (**Fig. 4b**). Again, photosynthesis (as well as ribosome assembly) genes were enriched among the down-regulated genes. Together, this supports the model that the nucleus recognizes $^1O_2$ as a specific chloroplast signal and regulates chloroplast function accordingly, possibly as a means to mitigate further production of ROS. This effect was partly dependent on cytoplasmic PUB4, supporting the existence of a secondary signal being involved in the propagation of a $^1O_2$ signal (**Figs. 2a and 4b**). Interestingly, PPEGs involved in chloroplast development (e.g., plastid gene expression, plastid protein import) were upregulated in *fc2 pub4* mutants in cycling light conditions (**Fig. S7d**), suggesting that these chloroplasts may have increased protein turnover that could offer protection from photo-oxidative damage.

$^1O_2$ accumulation due to a far-red block of chloroplast development was also reported to repress photosynthesis genes (Page et al., 2017), further supporting a signaling role for $^1O_2$ to limit photosynthesis. However, the far-red block signal was dependent on *EXECUTOR1* (*EX1*) and *EX2*, which are dispensable in adult *fc2* plants (Tano et al., 2023), suggesting that multiple $^1O_2$ signals impact photosynthetic gene expression.

<u>Transcription factor networks are involved in propagating the singlet oxygen signal</u>

The large change in $^1O_2$-induced gene expression correlated with the induction of WRKY, ERF, and NAC TF families (**Figs. S4a and b**), consistent with stress responses involving SA and JA (Javed et al., 2020) and the induction of leaf senescence (Cao et al., 2023). A complimentary TFEA analysis was used to determine which transcription factors were responsible for the observed DEGs and confirmed that the WRKY and NAC TF families play important roles in propagating the $^1O_2$ signal (**Fig. S6c**). However, ERF targets were not found to be enriched, suggesting that this class of TFs may not be as active during $^1O_2$ signaling.

The TFEA also revealed some insight into the role of PUB4 in signaling. Both NAC TF transcripts and NAC family target transcripts are reversed by *pub4*, indicating that such NAC TF networks may regulate $^1O_2$-induced PCD or senescence (**Fig. S6c**). However, the induction of WRKY targets is only modestly affected by *pub4*, despite the reversal of WRKY TF transcript accumulation. This suggests that $^1O_2$ affects WRKY function independently from PUB4. One of the WRKYs still active in *fc2 pub4* is WRKY33, which has been reported to play a role in defense against necrotrophic pathogens by regulating crosstalk between SA- and JA-response pathways (Zheng et al., 2006; Zhou et al., 2014) and is an early $^1O_2$ response gene (Dogra et al., 2017). Another, WRKY40, may be involved in the EX1-dependent regulation of regulate $^1O_2$-responsive genes (Li et al., 2023). Thus, some PUB4-independent $^1O_2$ signaling occurs through WRKYs, but it does not trigger PCD. Such signaling could possibly occur through the production of β-cyclocitral (β-cc), a β-carotene oxidation product, that can induce a $^1O_2$ retrograde signal, but without PCD (Ramel et al., 2012). Thus, $^1O_2$ may initiate the induction of parallel signals involving distinct sets of TFs, with only part of this signal being dependent on PUB4 and leading to PCD.

Jasmonic acid synthesis is the result, rather than the cause, of singlet oxygen signaling

An analysis of the genes upregulated in *fc2* during $^1O_2$ stress showed an enrichment for JA biosynthesis, JA signaling, and senescence (**Fig. 3a**), and *fc2* mutants specifically accumulated JA under cycling light conditions (**Fig. 6b**). We initially hypothesized that this high level of JA may be associated with $^1O_2$-induced PCD in *fc2* plants as JA can induce the onset of senescence (He et al., 2002; Shan et al., 2011; Zhang et al., 2020) and *pub4* blocked the accumulation of JA (**Fig. 6b**). However, blocking JA synthesis in *fc2 aos* seedlings only mildly reduced PCD (**Figs. 7a and b**) and it had no obvious effect in adult plants (**Figs. 7 c, g, h, and i**). This suggested that in *fc2* mutants, JA is produced in response to $^1O_2$ or PCD, rather than being directly responsible for $^1O_2$ signaling and PCD. In this case, JA may be acting similarly to its role during wounding (or herbivory) to signal for a defense response (Koo and Howe, 2009). Interestingly, such mechanical damage can produce $^1O_2$ in a light-independent mechanism (Flors et al., 2006), but the signaling role this source of $^1O_2$ has not been well-studied.

The role of JA in promoting $^1O_2$-induced PCD has been previously investigated, but with conflicting results. The EL-induced PCD phenotype of adult *ch1* mutant plants is blocked by an *aos* mutation (*dde2-2*), suggesting that JA synthesis was required for $^1O_2$-induced lesion formation (Ramel et al., 2013). However, blocking JA production in the $^1O_2$ accumulating *flu* mutant with the *aos* mutation leads to increased PCD in adult plants (Przybyla et al., 2008). Finally, blocking JA synthesis with the *opr3* mutation reduces $^1O_2$-induced PCD in protoplasts (Danon et al., 2005), although *opr3* leads to the accumulation of the intermediate OPDA, which has signaling properties (Jimenez Aleman et al., 2022). Another study has suggested that the role of JA in promoting PCD after EL stress can be reversed under simultaneous heat stress, suggesting there is cross-talk between ROS and heat stress pathways (Balfagón et al., 2019).

Together, these results argue against a simple model in which JA is directly responsible for $^1O_2$-induced PCD. Instead, the effect of JA on PCD may be context specific and influenced by life stage, temperature, and/or OPDA levels.

The *pub4* mutant is tolerant to singlet oxygen due to elevated SA content

fc2 mutants also accumulate SA under cycling light conditions (**Fig. 8d**). Based on our expression data, this SA is likely from the ICS pathway where *ICS1*, rather than the *PALs* (**Figs. 8a and b**), is responsible for producing the majority of SA in Arabidopsis (Wildermuth et al., 2001). As SA plays a pivotal role in orchestrating the plant's response to biotic and abiotic stress (Yang et al., 2023), it can affect PCD responses. For instance, elevated levels of SA were observed in lesion-mimic mutants and can trigger hypersensitive response (HR) and PCD (Radojičić et al., 2018), potentially serving as a strategy to restrict the proliferation of pathogens during infection (Brodersen et al., 2005). However, our understanding of the specific role of SA in $^1O_2$-triggered PCD remains unclear.

Reducing SA content in *fc2* with the *eds16* mutation did not reduce $^1O_2$-triggered PCD, arguing against a pro-PCD role for this hormone (**Figs. 9d, g, and i**). Instead, the *eds16* mutation enhanced growth defects in *fc2* (**Figs. 9j and k**) indicating that SA may offer protection from $^1O_2$ stress. Indeed, *fc2 pub4* mutants exhibited elevated levels of SA (**Fig. 9a**), which was responsible for several of this mutant's phenotypes. Lowering SA levels with the *eds16* mutation restored PCD, chlorophyll content, and growth in *fc2 pub4* that was comparable to *fc2* (**Figs. 10a, b, d-f, g, and h**). This protection extended beyond the conditional *fc2* PCD phenotype, as the *eds16* mutation also reduced the ability of *fc2 pub4* to tolerate EL stress, which is a natural way to induce $^1O_2$ accumulation in the chloroplast (Triantaphylides et al., 2008) (**Figs. 10i and j**).

However, high SA content alone does not seem sufficient to lead to a "*pub4* phenotype", as spaying *fc2* plants with SA did not reduce PCD despite a strong SA transcriptional response (**Figs. S12a-f**). Notably, the *pub4-2* loss-of-function allele also leads to elevated SA content and signaling (Desaki et al., 2019), yet this allele cannot suppress PCD in *fc2* (Woodson et al., 2015). This difference is likely due to amino acid substitution caused by the *pub4-6* allele (G255R), which affects a conserved residue in the U-Box and likely renders this domain inactive. Thus, a mutant protein is produced that cannot interact with an E2 and transfer ubiquitin to a target protein. Expressing PUBs without a functional U-Box can negatively affect the ubiquitination system (Zhou et al., 2015a), possibly by interfering with related protein family members. As such, we hypothesize that the lack of PUB4 activity leads to high SA levels, but the specific *pub4-6* allele also leads to a gain-of-function effect that is necessary to block $^1O_2$ signaling.

What additional role may PUB4 have in $^1O_2$ signaling? We show that *pub4-6* leads to constitutive anthocyanin production, but this phenotype is not correlated to PCD (**Figs. S13a, b, and d**). PUB4 may modulate $^1O_2$ signaling and PCD by altering the ratio of JA and SA (i.e., high SA and low JA) (**Figs. 9a and b**). Both JA and SA hormones are central to plant defense and influence each other reciprocally to enable the plant to make appropriate strategies to defend itself and acclimatize (Tamaoki et al., 2013). Thus, it may be that $^1O_2$ signaling requires a certain ratio of JA and SA levels and or signaling to be active, which the *pub4* mutation can achieve by the simultaneous regulation of both pathways. Alternatively, *pub4* may achieve a similar scenario by blocking JA signaling. In detached leaf assays, *pub4* blocked MeJA-induced senescence in the dark (**Figs. 5b-d**), suggesting that PUB4 also work downstream of JA accumulation. This agrees with the observation that *pub4* blocked protein ubiquitination in senescing leaves lacking autophagy machinery (Kikuchi et al., 2020).

It is not clear why *pub4* mutants accumulate high levels of SA. Transcripts of SA biosynthesis genes are only modestly increased in *fc2 pub4*, so it is tempting to speculate that PUB4 targets an enzyme involved in SA metabolism and regulates this pathway at a post-translational level. However, no PUB4 ubiquitination targets have been identified. This is surprising considering PUB4 has been shown to have ubiquitination activity in vitro (Wang et al., 2013) and is involved in multiple (and seemingly incompatible) cellular processes including stress signaling (Woodson et al., 2015; Jeran et al., 2021), pollen development (Wang et al., 2013), meristem development (Kinoshita et al., 2015), and pattern triggered immunity (Wang et al., 2022; Yu et al., 2022). Our results suggest that the constitutive activation of SA synthesis and signaling may be an underlying mechanism by which *pub4* mutations affect these processes, which can be regulated, at least in part, by SA. Thus, PUB4 may sit at a hub of intracellular signaling networks influencing cell decisions through multiple mechanisms including the regulation of stress hormone synthesis and signaling.

4. Materials and Methods

4.1 Plant material and growth conditions

The *Arabidopsis thaliana* ecotype Columbia-0 was used as wild type (wt). Supplementary **Table S26** lists the mutant lines used. Mutant line *fc2-1* (GABI_766H08) (Woodson et al., 2011) and *aos1-1*/*dde2* (SALK_017756) (Przybyla et al., 2008) came from the GABI-Kat (Kleinboelting et al., 2012) and SALK T-DNA (Alonso et al., 2003) collections, respectively. *eds16-1*/*sid2-2* (Wildermuth et al., 2001) was obtained from the Arabidopsis Biological Resource Center (Columbus, OH) (CS16438), and *fc2-1 pub4-6* was previously described (Woodson et al., 2015). The higher-order mutants *fc2 eds16*, *fc2 aos*, and *fc2 pub4*

eds16 were generated via crossing and confirmed by genotyping. **Table S27** lists the primers used. The *aos* mutants have male-sterile phenotypes and do not produce siliques, which was rescued by exogenous application of 1 mM MeJA every other day (Park et al., 2002).

Seeds were sterilized using 30% liquid bleach (v/v) with 0.04% Triton X-100 (v/v) for 5 min, washed three times with sterile water, and resuspended in a 0.1% agar solution. Resuspended seeds were spread on plates containing Linsmaier and Skoog medium pH 5.7 (Caisson Laboratories, North Logan, UT, USA) with 0.6% micropropagation type-1 agar powder. Following 3-5 day stratification at 4°C in the dark, seeds were germinated in either 24h constant light (permissive) conditions or 6h light / 18h dark cycling light (stress conditions) at 120 µmol photons m^{-2} sec^{-1} at 21°C in fluorescent light chambers (Percival model CU-36L5).

For adult plant experiments, seven-day-old plants grown in 24h constant light conditions were transferred to PRO-MIX LP15 soil and growth was continued under the same growth conditions in a fluorescent reach-in plant growth chamber (Conviron). To induce $^1O_2$ stress, adult plants were either shifted to cycling light conditions (16h light / 8h dark) or subjected to a shift in light intensity. In the latter case, plants were shifted to constant dim light (~ 0.4 photons µmol m^{-2} sec^{-1}) for 8h and returned to full light (120 µmol photons m^{-2} sec^{-1}). Three-week old plants grown in 24h light conditions were sprayed with 0.015% Silwet 77 with or without 4 mM SA for SA treatments. Plants were kept in 24h light for one day before being shifted to cycling light conditions for three days.

For Excess light (EL) stress treatments, plants were treated and assessed as previously described (Lemke and Woodson, 2024) (**Supplementary Methods 1**).

4.2 RNA-Seq analyses

For whole transcriptome RNA-Seq analyses, plants were grown under 24h constant light conditions for 16 days. One set of plants was then shifted to cycling light conditions (16h light / 8h dark) for two days. Total leaf tissue was collected from 18-day-old plants one hour after subjective dawn. Samples were collected in biological triplicates, each replicate consisting of leaves pooled from three plants. Total RNA was extracted using the RNeasy Plant Mini Kit (Qiagen) and residual DNA was removed with the RNase-Free DNase Kit (Qiagen). A Qubit 2.0 Fluorometer was used to calculate RNA concentration and 4 mg of total RNA was used to prepare libraries with the TruSeq Stranded mRNA Library Prep Kit (Illumina, San Diego, US). Single-end sequencing (50bp) was performed on an Illumina HiSeq 2500.

4.3 Identification of differentially expressed genes and gene expression analysis

Single end 50bp reads were aligned to the Arabidopsis TAIR10 genome using the HISAT2 pipeline on RMTA (Read Mapping, Transcript Assembly) available through CyVerse's Discovery Environment (Peri et al., 2020). HISAT2 (v2.1.0) was used to align sequencing reads. Reads were assembled into transcripts using StringTie (v1.3.4). Annotation was conducted using TAIR10 FASTA sequence the TAIR10 genome GTF annotation file (www.arabidopsis.org).

The “feature_counts.txt” file obtained from RMTA was used as input for differential gene expression statistical analyses utilizing R studio-DESeq2 available through CyVerse. The DESeq2 was performed between samples (i.e., wt vs. mutants in 24 or cycling light conditions). Genes with a Log_2 fold-change > +/- 1.5 and a P*adj* < 0.01 were considered differentially expressed genes (DEGs) (**Tables S1-5**).

Heatmaps were generated using ClustalVis on https://biit.cs.ut.ee/clustvis/ (Metsalu and Vilo, 2015), and the heat mapper package (https://github.com/WishartLab/heatmapper) on

http://www.heatmapper.ca/ (Babicki et al., 2016), using Log_2 Fold-change values. Average linkage was used for the clustering method and Pearson correlation was used for the distance measurement method. Venn Diagrams comparing the number of DEGs across the four datasets were created using VENNY 2.1 (https://bioinfogp.cnb.csic.es/tools/venny/). To assess the impact of a genotype or condition on certain processes, DEGs were compared to lists of genes involved in senescence (**Table S21**), JA-related processes (Kim et al., 2015) (**Table S22**), SA-related processes (**Table S23**) and anthocyanin-related processes (**Table S25**), which were manually curated from the literature (Dempsey et al., 2011; Shin et al., 2013; Wasternack and Hause, 2013; Seyfferth and Tsuda, 2014; Shi and Xie, 2014; Lefevere et al., 2020; Khusnutdinov et al., 2021; Nomoto et al., 2021).

Gene Ontology (GO) enrichment analyses were performed for the up- and down-regulated DEGs for each dataset using ShinyGO 0.80 (http://bioinformatics.sdstate.edu/go/). The significantly enriched Gene Ontology (GO) terms were determined using default settings and a p-value threshold of ≤ 0.01 (**Tables S6, S7, S9, S10, and S20**).

4.4 Transcription factor analysis

Detailed methods used for transcription factor analyses may be found in **Supplemental Methods 2**. Briefly, DEGs identified in RNAseq data using a log_2FC +/- > 1, adjusted p-value ≤ 0.01 cutoff were to identify differentially expressed transcription factors and transcription factors with target genes enriched in these data. Hypergeometric tests were used to identify the enrichment of transcription factor families. Data used to generate heatmaps may be found in **Table S28.** Differentially expressed TFs (DETFs) were identified from DEG lists using PlantTFDB, were compiled (**Table S11 and S12**) and the counts for each family of TF were

determined (**Table S13**). GO enrichment analyses were used to identify the enrichment of Biological GO terms represented both in full DETF lists and sub-lists of the different TF families that were significantly enriched in our TF enrichment analysis (**Table S15**). A list of TFs whose targets were overrepresented in DEG lists was obtained from the TF enrichment tool on http://plantregmap.gao-lab.org/tf_enrichment.php (**Table S16**) and the counts for each TF family represented were determined (**Table S13**). Assessment of False Discovery Rate (FDR) for each TF family identified (**Table S17**).

4.5 RNA extraction, cDNA synthesis, and real-time quantitative PCR

Measurement of steady-state RNA transcripts were made as previously described (Alamdari et al., 2020) (**Supplementary Methods 3**). **Table S27** lists the primers used.

4.6 DNA extraction and PCR genotyping

To genotype mutant lines, genomic DNA was extracted using a CTAB-based protocol (Healey et al. 2014). PCR was performed as previously described (Lemke et al., 2021). **Table S27** lists the primers used.

4.7 Measuring leaf area and chlorophyll content

Leaf area was determined by photographing all leaves in the rosette and calculating total area using ImageJ. Plant chlorophyll content was extracted from total leaf tissue and measured spectrophotometrically according to (Arnon, 1949) as previously described (Woodson et al., 2015).

4.8 Cell death measurements

Cell death was measured in adult plants and seedlings, using trypan blue staining as previously described (Woodson et al., 2015).

4.9 Anthocyanin measurements

One-week-old seedlings were harvested, weighed, frozen in liquid N_2, and ground to a fine powder. Anthocyanin measurements were performed as described (Neff and Chory, 1998) (**Supplemental Methods 4**).

4.10 Leaf senescence assay

The third and fourth rosette leaves from 3-week-old plants were floated on 3 mL of distilled water with or without 100 mM methyl-jasmonate (MeJA). Samples were then incubated in the dark at 21°C for 3 days.

4.11 Jasmonic acid and Salicylic acid measurements

SA and JA were extracted from whole rosettes analyzed as previously described (Jiang et al., 2019; Zeng et al., 2022). Plants were grown in 24h constant light for 17 days, and one set of plants were then shifted to 16h light/8h dark diurnal cycling light. Samples were collected two days later, 3hrs after subjective dawn.

4.12 Protein extraction and immunoblot analyses

Total leaf tissue from plants was collected one hour after subjective dawn, frozen in liquid N_2, and homogenized in extraction buffer (50 mM Tris-Cl pH 8.0, 150 mM NaCl, 0.5%

Nonidet P-40 (v:v), and protease inhibitors (Roche)). Cell debris was removed by centrifugation at 10,000 x g for 20 min at 4^0C. Total protein concentration was measured using the Bradford assay (BioRad) and 15ug of each sample was loaded into a 4-20% SDS-PAGE precast protein gel (BioRad). Proteins were fractionated by electrophoresis and then transferred to PVDF membranes (BioRad). Membranes were incubated with specific primary and secondary antibodies. Immunoblots were imaged by chemiluminescence with the ProSignal Pico ECL Reagents (Genesee Scientific) on a ChemiDoc (Bio-Rad). Polyclonal GFP and Actin antibodies were purchased from BioRad Laboratories. Polyclonal antibodies for NAD(P)H dehydrogenase subunit 45 (NDH45), Thylakoid Membrane Cytochrome B6 Protein (PetB), ATP Synthase Gamma Chain (AtpC), and Rubisco large subunit (RBCL) were purchased from PhytoAB (California, USA). Antibodies for photosystem I core protein (PsaA) and D2 protein of PSII (PsbD) were purchased from Agrisera (Vännäs, Sweden).

4.13 Biomass measurements

Fresh weight was measured in three-week-old plants. For dry weight measurements, samples were stored in envelopes and desiccated at 65°C for 48 hours.

Declarations

Availability of data and materials

Raw sequencing data will be made available in a public online data repository after peer review and upon publication of this study. All other data is included in the manuscript or Supplementary Material. Further inquiries can be directed to the corresponding author.

Competing interests

The authors declare that they have no competing interests.

Funding

The authors acknowledge the Division of Chemical Sciences, Geosciences, and Biosciences, Office of Basic Energy Sciences of the U.S. Department of Energy grant DE-SC0019573 awarded to J.D.W., and National Institutes of Health (NIH) grant R01GM107311-8 and National Science Foundation (NSF) grant 2104365 awarded to K.D. M.D.L was supported by the NIH T32 GM136536 training grant and the UA Richard A. Harvill Graduate Fellowship. The funding bodies played no role in the design of the study and collection, analysis, and interpretation of data and in writing the manuscript.

Authors' contributions

SR and JDW planned and designed the research. SR performed RNA-Seq data analysis, created higher-order mutants, performed genotyping, phenotyping, biochemical assays, cell death measurements, and immunoblotting. MDL assisted with processing RNA-seq data, performed transcription factor analyses, performed SA-treatment RT-qPCR, and performed EL stress treatments. AMA assisted with genotyping and the leaf senescence assay. MFGM and KD measured JA and SA content. JDW conceived the original scope of the project and managed the project. SR, MDL, MFGM, KD, and JDW contributed to data analysis and interpretation, and reviewed the manuscript. SR, MDL, and JDW wrote the manuscript. All authors approved the final version.

Acknowledgments

The authors thank Kamran Alamdari (University of Arizona) for technical assistance with RNA extractions and RT-qPCR analyses, and Sophia Daluisio and Alexa Abate (University of Arizona) for technical assistance with plant maintenance.

Short legends for supporting information

Supplemental Figures

Figure S1. Visualization of variance among RNA-seq replicates used in the study.

Figure S2. Volcano plot analysis of mean differential gene expression between genotypes in a single condition.

Figure S3. Gene ontology analyses of differentially expressed genes.

Figure S4. WRKY, ERF, and NAC transcription factor networks are induced by chloroplast singlet oxygen accumulation.

Figure S5. Gene Ontology term enrichment of differentially expressed transcription factors genes and transcription factor gene families.

Figure S6. WRKY and NAC transcription factor targets are induced by chloroplast singlet oxygen accumulation and activation of NAC targets is blocked by the *pub4* mutation.

Figure S7. Gene ontology analyses of differentially expressed plastid protein-encoding genes.

Figure S8. Relative expression of plastid protein-encoding genes during singlet oxygen stress.

Figure S9. Activation of senescence pathways is blocked by the *pub4* mutation.

Figure S10. Testing the effect of the *aos* mutation on *fc2* phenotypes.

Figure S11. Testing the effect of the *eds16* mutation on *fc2* phenotypes.

Figure S12. Application of Salicylic acid does not reverse lesion formation in *fc2* mutants.

Figure S13. *fc2 pub4* mutants accumulate anthocyanin, but it is not responsible for blocking singlet-oxygen-induced cell death.

Supplementary Methods

Methods 1. Excess light treatments

Methods 2. Transcription factor analysis

Methods 3. RNA extraction, cDNA synthesis, and real-time quantitative PCR.

Methods 4. Anthocyanin measurements

Supplementary Notes

Note 1. Analysis of anthocyanin-related gene expression.

Supplemental Tables

Table S1. All differentially expressed genes identified from the RNA-seq data set by pairwise comparisons between mutants and wild type within one condition

Table S2. All differentially expressed genes identified between wt and *fc2* under constant light conditions

Table S3. All differentially expressed genes identified between wt and *fc2* under cycling light conditions

Table S4. All differentially expressed genes identified between wt and *fc2 pub4* under constant light conditions

Table S5. All differentially expressed genes identified between wt and *fc2 pub4* under cycling light conditions

Table S6. Gene Ontology term enrichment of DEGs identified between wt and *fc2* in constant light conditions

Table S7. Gene Ontology term enrichment of DEGs identified between wt and *fc2* in cycling light conditions

Table S8. Differentially expressed genes that are unique or shared among *fc2* and *fc2 pub4*

Table S9. Gene Ontology term enrichment of DEGs associated with *fc2 pub4* in constant light conditions

Table S10. Gene Ontology term enrichment of DEGs associated with *fc2 pub4* in cycling light conditions

Table S11. Differentially Expressed Gene Lists with relaxed cutoffs

Table S12. Identification of differentially expressed transcription factors

Table S13. Quantification of differentially expressed transcription factors among the pairwise comparisons

Table S14. Enrichment analysis of differentially expressed transcription factors

Table S15. Gene ontology term enrichment analysis of differentially expressed transcription factors

Table S16. Transcription factor enrichment analysis of differentially expressed genes

Table S17. Enrichment analysis of transcription factors whose targets are represented in differentially expressed gene lists

Table S18. Comparison of transcription factors (TFs) identified in differentially expressed TF (DETF) and TF enrichment analysis (TFEA)

Table S19. The differentially expressed plastid protein-encoding genes identified in the RNA-seq dataset

Table S20. Gene Ontology term enrichment of differentially expressed plastid protein-encoding genes

Table S21. Analysis of the response of senescence-related genes to singlet oxygen stress

Table S22. Jasmonic acid-related genes analyzed in this study

Table S23. Salicylic acid-related genes analyzed in this study

Table S24. Assessing the Salicylic acid transcriptional response in *fc2 pub4* mutants

Table S25. Assessing the biosynthesis of anthocyanin and its regulation in the RNA-seq data set

Table S26. Mutant plant lines used in study

Table S27. List of primers used for RT-qPCR and Genotyping.

Table S28. Expression matrix used to generate Differentially Expressed Transcription Factor heatmap

References

Alamdari, K., Fisher, K.E., Sinson, A.B., Chory, J., and Woodson, J.D. (2020). Roles for the chloroplast-localized PPR Protein 30 and the "Mitochondrial" Transcription Termination Factor 9 in chloroplast quality control. Plant J **103,** 735-751.

Alonso, J.M., Stepanova, A.N., Leisse, T.J., Kim, C.J., Chen, H., Shinn, P., Stevenson, D.K., Zimmerman, J., Barajas, P., Cheuk, R., Gadrinab, C., Heller, C., Jeske, A., Koesema, E., Meyers, C.C., Parker, H., Prednis, L., Ansari, Y., Choy, N., Deen, H., Geralt, M., Hazari, N., Hom, E., Karnes, M., Mulholland, C., Ndubaku, R., Schmidt, I., Guzman, P., Aguilar-Henonin, L., Schmid, M., Weigel, D., Carter, D.E., Marchand, T., Risseeuw, E., Brogden, D., Zeko, A., Crosby, W.L., Berry, C.C., and Ecker, J.R. (2003). Genome-wide insertional mutagenesis of Arabidopsis thaliana. Science **301,** 653-657.

Arnon, D.I. (1949). Copper Enzymes in Isolated Chloroplasts. Polyphenoloxidase in Beta Vulgaris. Plant Physiol **24,** 1-15.

Babicki, S., Arndt, D., Marcu, A., Liang, Y., Grant, J.R., Maciejewski, A., and Wishart, D.S. (2016). Heatmapper: web-enabled heat mapping for all. Nucleic acids research **44,** W147-W153.

Balfagón, D., Sengupta, S., Gómez-Cadenas, A., Fritschi, F.B., Azad, R.K., Mittler, R., and Zandalinas, S.I. (2019). Jasmonic Acid Is Required for Plant Acclimation to a Combination of High Light and Heat Stress. Plant Physiol **181,** 1668-1682.

Beaugelin, I., Chevalier, A., D'Alessandro, S., Ksas, B., Novák, O., Strnad, M., Forzani, C., Hirt, H., Havaux, M., and Monnet, F. (2019). OXI1 and DAD Regulate Light-Induced Cell Death Antagonistically through Jasmonate and Salicylate Levels. Plant Physiol **180,** 1691-1708.

Beyer, S.F., Bel, P.S., Flors, V., Schultheiss, H., Conrath, U., and Langenbach, C.J.G. (2021). Disclosure of salicylic acid and jasmonic acid-responsive genes provides a molecular tool for deciphering stress responses in soybean. Scientific Reports **11,** 20600.

Breeze, E. (2019). Master MYCs: MYC2, the Jasmonate Signaling "Master Switch". Plant Cell **31,** 9-10.

Bresson, J., Bieker, S., Riester, L., Doll, J., and Zentgraf, U. (2018). A guideline for leaf senescence analyses: from quantification to physiological and molecular investigations. J Exp Bot **69,** 769-786.

Brodersen, P., Malinovsky, F.G., Hématy, K., Newman, M.A., and Mundy, J. (2005). The role of salicylic acid in the induction of cell death in Arabidopsis acd11. Plant Physiol **138,** 1037-1045.

Cao, J., Liu, H., Tan, S., and Li, Z. (2023). Transcription Factors-Regulated Leaf Senescence: Current Knowledge, Challenges and Approaches. Int J Mol Sci **24**.

Chan, K.X., Mabbitt, P.D., Phua, S.Y., Mueller, J.W., Nisar, N., Gigolashvili, T., Stroeher, E., Grassl, J., Arlt, W., Estavillo, G.M., Jackson, C.J., and Pogson, B.J. (2016). Sensing and signaling of oxidative stress in chloroplasts by inactivation of the SAL1 phosphoadenosine phosphatase. Proc Natl Acad Sci U S A **113,** E4567-4576.

Chow, K.S., Singh, D.P., Walker, A.R., and Smith, A.G. (1998). Two different genes encode ferrochelatase in Arabidopsis: mapping, expression and subcellular targeting of the precursor proteins. Plant J **15,** 531-541.

Christiansen, M.W., and Gregersen, P.L. (2014). Members of the barley NAC transcription factor gene family show differential co-regulation with senescence-associated genes during senescence of flag leaves. J Exp Bot **65,** 4009-4022.

D'Alessandro, S., Beaugelin, I., and Havaux, M. (2020). Tanned or Sunburned: How Excessive Light Triggers Plant Cell Death. Mol Plant **13,** 1545-1555.

Danon, A., Miersch, O., Felix, G., Camp, R.G., and Apel, K. (2005). Concurrent activation of cell death-regulating signaling pathways by singlet oxygen in *Arabidopsis thaliana*. The Plant Journal **41,** 68-80.

Dempsey, D.A., Vlot, A.C., Wildermuth, M.C., and Klessig, D.F. (2011). Salicylic Acid biosynthesis and metabolism. Arabidopsis Book **9,** e0156.

Desaki, Y., Takahashi, S., Sato, K., Maeda, K., Matsui, S., Yoshimi, I., Miura, T., Jumonji, J.I., Takeda, J., Yashima, K., Kohari, M., Suenaga, T., Terada, H., Narisawa, T., Shimizu, T., Yumoto, E., Miyamoto, K., Narusaka, M., Narusaka, Y., Kaku, H., and Shibuya, N. (2019). PUB4, a CERK1-Interacting Ubiquitin Ligase, Positively Regulates MAMP-Triggered Immunity in Arabidopsis. Plant and Cell Physiology **60,** 2573-2583.

Dogra, V., and Kim, C. (2019). Singlet Oxygen Metabolism: From Genesis to Signaling. Front Plant Sci **10,** 1640.

Dogra, V., Duan, J., Lee, K.P., Lv, S., Liu, R., and Kim, C. (2017). FtsH2-Dependent Proteolysis of EXECUTER1 Is Essential in Mediating Singlet Oxygen-Triggered Retrograde Signaling in *Arabidopsis thaliana*. Front Plant Sci **8,** 1145.

Dong, J., Chen, C., and Chen, Z. (2003). Expression profiles of the Arabidopsis WRKY gene superfamily during plant defense response. Plant Mol Biol **51,** 21-37.

Fisher, K.E., Krishnamoorthy, P., Joens, M.S., Chory, J., Fitzpatrick, J.A.J., and Woodson, J.D. (2022). Singlet Oxygen Leads to Structural Changes to Chloroplasts During their Degradation in the *Arabidopsis thaliana plastid ferrochelatase two* Mutant. Plant and Cell Physiology **63,** 248-264.

Flors, C., Fryer, M.J., Waring, J., Reeder, B., Bechtold, U., Mullineaux, P.M., Nonell, S., Wilson, M.T., and Baker, N.R. (2006). Imaging the production of singlet oxygen in vivo using a new fluorescent sensor, Singlet Oxygen Sensor Green. J Exp Bot **57,** 1725-1734.

He, Y., Fukushige, H., Hildebrand, D.F., and Gan, S. (2002). Evidence supporting a role of jasmonic acid in Arabidopsis leaf senescence. Plant Physiol **128,** 876-884.

Hu, Y., Jiang, Y., Han, X., Wang, H., Pan, J., and Yu, D. (2017). Jasmonate regulates leaf senescence and tolerance to cold stress: crosstalk with other phytohormones. J Exp Bot **68,** 1361-1369.

Huang, W., Wang, Y., Li, X., and Zhang, Y. (2020). Biosynthesis and Regulation of Salicylic Acid and N-Hydroxypipecolic Acid in Plant Immunity. Mol Plant **13,** 31-41.

Javed, T., Shabbir, R., Ali, A., Afzal, I., Zaheer, U., and Gao, S.J. (2020). Transcription Factors in Plant Stress Responses: Challenges and Potential for Sugarcane Improvement. Plants (Basel) **9**.

Jeran, N., Rotasperti, L., Frabetti, G., Calabritto, A., Pesaresi, P., and Tadini, L. (2021). The PUB4 E3 Ubiquitin Ligase Is Responsible for the Variegated Phenotype Observed upon Alteration of Chloroplast Protein Homeostasis in Arabidopsis Cotyledons. Genes **12,** 1387.

Jiang, J., Zeng, L., Ke, H., De La Cruz, B., and Dehesh, K. (2019). Orthogonal regulation of phytochrome B abundance by stress-specific plastidial retrograde signaling metabolite. Nat Commun **10,** 2904.

Jimenez Aleman, G.H., Thirumalaikumar, V.P., Jander, G., Fernie, A.R., and Skirycz, A. (2022). OPDA, more than just a jasmonate precursor. Phytochemistry **204,** 113432.

Jin, J., Zhang, H., Kong, L., Gao, G., and Luo, J. (2014). PlantTFDB 3.0: a portal for the functional and evolutionary study of plant transcription factors. Nucleic Acids Res **42,** D1182-1187.

Jin, J., Tian, F., Yang, D.C., Meng, Y.Q., Kong, L., Luo, J., and Gao, G. (2017). PlantTFDB 4.0: toward a central hub for transcription factors and regulatory interactions in plants. Nucleic Acids Res **45,** D1040-D1045.

Kazan, K., and Manners, J.M. (2013). MYC2: the master in action. Mol Plant **6,** 686-703.

Kazan, K., and Lyons, R. (2014). Intervention of Phytohormone Pathways by Pathogen Effectors. Plant Cell **26,** 2285-2309.

Kennedy, J.C., and Pottier, R.H. (1992). Endogenous protoporphyrin IX, a clinically useful photosensitizer for photodynamic therapy. Journal of photochemistry and photobiology. B, Biology **14,** 275-292.

Khusnutdinov, E., Sukhareva, A., Panfilova, M., and Mikhaylova, E. (2021). Anthocyanin Biosynthesis Genes as Model Genes for Genome Editing in Plants. Int J Mol Sci **22**.

Kikuchi, Y., Nakamura, S., Woodson, J.D., Ishida, H., Ling, Q., Hidema, J., Jarvis, R.P., Hagihara, S., and Izumi, M. (2020). Chloroplast Autophagy and Ubiquitination Combine to Manage Oxidative Damage and Starvation Responses. Plant Physiol **183,** 1531-1544.

Kim, J., Chang, C., and Tucker, M.L. (2015). To grow old: regulatory role of ethylene and jasmonic acid in senescence. Front Plant Sci **6,** 20.

Kim, J., Kim, J.H., Lyu, J.I., Woo, H.R., and Lim, P.O. (2018). New insights into the regulation of leaf senescence in Arabidopsis. J Exp Bot **69,** 787-799.

Kinoshita, A., ten Hove, C.A., Tabata, R., Yamada, M., Shimizu, N., Ishida, T., Yamaguchi, K., Shigenobu, S., Takebayashi, Y., Iuchi, S., Kobayashi, M., Kurata, T., Wada, T., Seo, M., Hasebe, M., Blilou, I., Fukuda, H., Scheres, B., Heidstra, R., Kamiya, Y., and Sawa, S. (2015). A plant U-box protein, PUB4, regulates asymmetric cell division and cell proliferation in the root meristem. Development **142,** 444-453.

Kleinboelting, N., Huep, G., Kloetgen, A., Viehoever, P., and Weisshaar, B. (2012). GABI-Kat SimpleSearch: new features of the Arabidopsis thaliana T-DNA mutant database. Nucleic Acids Res **40,** D1211-1215.

Koo, A.J., and Howe, G.A. (2009). The wound hormone jasmonate. Phytochemistry **70,** 1571-1580.

Lai, Z., Li, Y., Wang, F., Cheng, Y., Fan, B., Yu, J.Q., and Chen, Z. (2011). Arabidopsis Sigma Factor Binding Proteins Are Activators of the WRKY33 Transcription Factor in Plant Defense. Plant Cell.

Lefevere, H., Bauters, L., and Gheysen, G. (2020). Salicylic Acid Biosynthesis in Plants. Front Plant Sci **11,** 338.

Lemke, M.D., and Woodson, J.D. (2022). Targeted for destruction: degradation of singlet oxygen-damaged chloroplasts. Plant Signal Behav **17,** 2084955.

Lemke, M.D., and Woodson, J.D. (2024). A genetic screen for dominant chloroplast reactive oxygen species signaling mutants reveals life stage-specific singlet oxygen signaling networks. Front Plant Sci **14**.

Lemke, M.D., Fisher, E.M., Kozlowska, M.A., Tano, D.W., and Woodson, J.D. (2021). The core autophagy machinery is not required for chloroplast singlet oxygen-mediated cell death in the Arabidopsis *plastid ferrochelatase two* mutant. BMC Plant Biol **21,** 342.

Li, Y., Liu, H., Ma, T., Li, J., Yuan, J., Xu, Y.C., Sun, R., Zhang, X., Jing, Y., Guo, Y.L., and Lin, R. (2023). Arabidopsis EXECUTER1 interacts with WRKY transcription factors to mediate plastid-to-nucleus singlet oxygen signaling. Plant Cell **35,** 827-851.

Mei, Y., Hu, T., Wang, Y., Lozano-Durán, R., Yang, X., and Zhou, X. (2023). Two viral proteins translated from one open reading frame target different layers of plant defense. Plant Commun**,** 100788.

Metsalu, T., and Vilo, J. (2015). ClustVis: a web tool for visualizing clustering of multivariate data using Principal Component Analysis and heatmap. Nucleic Acids Res **43,** W566-570.

Neff, M.M., and Chory, J. (1998). Genetic interactions between phytochrome A, phytochrome B, and cryptochrome 1 during Arabidopsis development. Plant Physiol **118,** 27-35.

Nomoto, M., Skelly, M.J., Itaya, T., Mori, T., Suzuki, T., Matsushita, T., Tokizawa, M., Kuwata, K., Mori, H., Yamamoto, Y.Y., Higashiyama, T., Tsukagoshi, H., Spoel, S.H., and Tada, Y. (2021). Suppression of MYC transcription activators by the immune cofactor NPR1 fine-tunes plant immune responses. Cell Rep **37,** 110125.

Ochsenbein, C., Przybyla, D., Danon, A., Landgraf, F., Göbel, C., Imboden, A., Feussner, I., and Apel, K. (2006). The role of EDS1 (enhanced disease susceptibility) during singlet oxygen-mediated stress responses of Arabidopsis. The Plant Journal **47,** 445-456.

Ogilby, P.R. (2010). Singlet oxygen: there is indeed something new under the sun. Chemical Society reviews **39,** 3181-3209.

Page, M.T., McCormac, A.C., Smith, A.G., and Terry, M.J. (2017). Singlet oxygen initiates a plastid signal controlling photosynthetic gene expression. New Phytologist **213,** 1168-1180.

Park, J.H., Halitschke, R., Kim, H.B., Baldwin, I.T., Feldmann, K.A., and Feyereisen, R. (2002). A knock-out mutation in allene oxide synthase results in male sterility and defective wound signal transduction in Arabidopsis due to a block in jasmonic acid biosynthesis. Plant J **31,** 1-12.

Peri, S., Roberts, S., Kreko, I.R., McHan, L.B., Naron, A., Ram, A., Murphy, R.L., Lyons, E., Gregory, B.D., Devisetty, U.K., and Nelson, A.D.L. (2020). Read Mapping and Transcript Assembly: A Scalable and High-Throughput Workflow for the Processing and Analysis of Ribonucleic Acid Sequencing Data. Fronteirs in Genetics **10**.

Pieterse, C.M.J., Van der Does, D., Zamioudis, C., Leon-Reyes, A., and Van Wees, S.C.M. (2012). Hormonal Modulation of Plant Immunity. Annu Rev Cell Dev Biol **28,** 489-521.

Przybyla, D., Gobel, C., Imboden, A., Hamberg, M., Feussner, I., and Apel, K. (2008). Enzymatic, but not non-enzymatic, $^1O_2$-mediated peroxidation of polyunsaturated fatty acids forms part of the EXECUTER1-dependent stress response program in the *flu* mutant of *Arabidopsis thaliana*. Plant J **54,** 236-248.

Qi, T., Wang, J., Huang, H., Liu, B., Gao, H., Liu, Y., Song, S., and Xie, D. (2015). Regulation of Jasmonate-Induced Leaf Senescence by Antagonism between bHLH Subgroup IIIe and IIId Factors in Arabidopsis. Plant Cell **27,** 1634-1649.

Radojičić, A., Li, X., and Zhang, Y. (2018). Salicylic Acid: A Double-Edged Sword for Programed Cell Death in Plants. Front Plant Sci **9,** 1133.

Ramel, F., Birtic, S., Ginies, C., Soubigou-Taconnat, L., Triantaphylides, C., and Havaux, M. (2012). Carotenoid oxidation products are stress signals that mediate gene responses to singlet oxygen in plants. Proc Natl Acad Sci U S A **109,** 5535-5540.

Ramel, F., Ksas, B., Akkari, E., Mialoundama, A.S., Monnet, F., Krieger-Liszkay, A., Ravanat, J.L., Mueller, M.J., Bouvier, F., and Havaux, M. (2013). Light-induced acclimation of the Arabidopsis *chlorina1* mutant to singlet oxygen. Plant Cell **25,** 1445-1462.

Reymond, P., and Farmer, E.E. (1998). Jasmonate and salicylate as global signals for defense gene expression. Curr Opin Plant Biol **1,** 404-411.

Seyfferth, C., and Tsuda, K. (2014). Salicylic acid signal transduction: the initiation of biosynthesis, perception and transcriptional reprogramming. Front Plant Sci **5,** 697.

Shan, X., Wang, J., Chua, L., Jiang, D., Peng, W., and Xie, D. (2011). The role of Arabidopsis Rubisco activase in jasmonate-induced leaf senescence. Plant Physiol **155,** 751-764.

Shi, M.Z., and Xie, D.Y. (2014). Biosynthesis and metabolic engineering of anthocyanins in Arabidopsis thaliana. Recent Pat Biotechnol **8,** 47-60.

Shin, D.H., Choi, M., Kim, K., Bang, G., Cho, M., Choi, S.B., Choi, G., and Park, Y.I. (2013). HY5 regulates anthocyanin biosynthesis by inducing the transcriptional activation of the MYB75/PAP1 transcription factor in Arabidopsis. FEBS Lett **587,** 1543-1547.

Sun, A.Z., and Guo, F.Q. (2016). Chloroplast Retrograde Regulation of Heat Stress Responses in Plants. Front Plant Sci **7,** 398.

Suo, J., Zhao, Q., David, L., Chen, S., and Dai, S. (2017). Salinity Response in Chloroplasts: Insights from Gene Characterization. International Journal of Molecular Sciences **18,** 1011.

Tamaoki, D., Seo, S., Yamada, S., Kano, A., Miyamoto, A., Shishido, H., Miyoshi, S., Taniguchi, S., Akimitsu, K., and Gomi, K. (2013). Jasmonic acid and salicylic acid activate a common defense system in rice. Plant Signal Behav **8,** e24260.

Tanaka, R., Kobayashi, K., and Masuda, T. (2011). Tetrapyrrole Metabolism in *Arabidopsis thaliana*. Arabidopsis Book **9,** e0145.

Tano, D.W., Kozlowska, M.A., Easter, R.A., and Woodson, J.D. (2023). Multiple pathways mediate chloroplast singlet oxygen stress signaling. Plant Molecular Biology **111,** 167-187.

Triantaphylides, C., and Havaux, M. (2009). Singlet oxygen in plants: production, detoxification and signaling. Trends Plant Sci **14,** 219-228.

Triantaphylides, C., Krischke, M., Hoeberichts, F.A., Ksas, B., Gresser, G., Havaux, M., Van Breusegem, F., and Mueller, M.J. (2008). Singlet oxygen is the major reactive oxygen species involved in photooxidative damage to plants. Plant Physiol **148,** 960-968.

Wagner, D., Przybyla, D., Op den Camp, R., Kim, C., Landgraf, F., Lee, K.P., Wursch, M., Laloi, C., Nater, M., Hideg, E., and Apel, K. (2004). The genetic basis of singlet oxygen-induced stress responses of *Arabidopsis thaliana*. Science **306,** 1183-1185.

Wang, H., Lu, Y., Jiang, T., Berg, H., Li, C., and Xia, Y. (2013). The Arabidopsis U-box/ARM repeat E3 ligase AtPUB4 influences growth and degeneration of tapetal cells, and its mutation leads to conditional male sterility. Plant J **74,** 511-523.

Wang, Y., Wu, Y., Yu, B., Yin, Z., and Xia, Y. (2017). EXTRA-LARGE G PROTEINs Interact with E3 Ligases PUB4 and PUB2 and Function in Cytokinin and Developmental Processes. Plant Physiol **173,** 1235-1246.

Wang, Y., Wu, Y., Zhong, H., Chen, S., Wong, K.B., and Xia, Y. (2022). Arabidopsis PUB2 and PUB4 connect signaling components of pattern-triggered immunity. New Phytol **233,** 2249-2265.

Wasternack, C., and Hause, B. (2013). Jasmonates: biosynthesis, perception, signal transduction and action in plant stress response, growth and development. An update to the 2007 review in Annals of Botany. Ann Bot **111,** 1021-1058.

Wildermuth, M.C., Dewdney, J., Wu, G., and Ausubel, F.M. (2001). Isochorismate synthase is required to synthesize salicylic acid for plant defence. Nature **414,** 562-565.

Woodson, J.D. (2022). Control of chloroplast degradation and cell death in response to stress. Trends in biochemical sciences **47,** 851-864.

Woodson, J.D., Perez-Ruiz, J.M., and Chory, J. (2011). Heme synthesis by plastid ferrochelatase I regulates nuclear gene expression in plants. Curr Biol **21,** 897-903.

Woodson, J.D., Joens, M.S., Sinson, A.B., Gilkerson, J., Salome, P.A., Weigel, D., Fitzpatrick, J.A., and Chory, J. (2015). Ubiquitin facilitates a quality-control pathway that removes damaged chloroplasts. Science **350,** 450-454.

Yang, W., Zhou, Z., and Chu, Z. (2023). Emerging Roles of Salicylic Acid in Plant Saline Stress Tolerance. Int J Mol Sci **24**.

Yu, G., Derkacheva, M., Rufian, J.S., Brillada, C., Kowarschik, K., Jiang, S., Derbyshire, P., Ma, M., DeFalco, T.A., Morcillo, R.J.L., Stransfeld, L., Wei, Y., Zhou, J.M., Menke, F.L.H., Trujillo, M., Zipfel, C., and Macho, A.P. (2022). The Arabidopsis E3 ubiquitin ligase PUB4 regulates BIK1 and is targeted by a bacterial type-III effector. Embo J **41,** e107257.

Zeng, L., Chen, H., Wang, Y., Hicks, D., Ke, H., Pruneda-Paz, J., and Dehesh, K. (2022). ORA47 is a transcriptional regulator of a general stress response hub. Plant J **110,** 562-571.

Zentgraf, U., Laun, T., and Miao, Y. (2010). The complex regulation of WRKY53 during leaf senescence of Arabidopsis thaliana. Eur J Cell Biol **89,** 133-137.

Zhang, Y., Ji, T.T., Li, T.T., Tian, Y.Y., Wang, L.F., and Liu, W.C. (2020). Jasmonic acid promotes leaf senescence through MYC2-mediated repression of CATALASE2 expression in Arabidopsis. Plant Sci **299,** 110604.

Zhang, Y., Xu, S., Ding, P., Wang, D., Cheng, Y.T., He, J., Gao, M., Xu, F., Li, Y., Zhu, Z., Li, X., and Zhang, Y. (2010). Control of salicylic acid synthesis and systemic acquired resistance by two members of a plant-specific family of transcription factors. Proc Natl Acad Sci U S A **107,** 18220-18225.

Zheng, Z., Qamar, S.A., Chen, Z., and Mengiste, T. (2006). Arabidopsis WRKY33 transcription factor is required for resistance to necrotrophic fungal pathogens. Plant Journal **48**.

Zhou, J., Wang, J., Yu, J.Q., and Chen, Z. (2014). Role and regulation of autophagy in heat stress responses of tomato plants. Front Plant Sci **5,** 174.

Zhou, J., Lu, D., Xu, G., Finlayson, S.A., He, P., and Shan, L. (2015a). The dominant negative ARM domain uncovers multiple functions of PUB13 in Arabidopsis immunity, flowering, and senescence. J Exp Bot **66,** 3353-3366.

Zhou, M., Wang, W., Karapetyan, S., Mwimba, M., Marqués, J., Buchler, N.E., and Dong, X. (2015b). Redox rhythm reinforces the circadian clock to gate immune response. Nature **523,** 472-476.

Zhuang, X., and Jiang, L. (2019). Chloroplast Degradation: Multiple Routes Into the Vacuole. Front Plant Sci **10,** 359.

Figure legends

Figure 1: The singlet oxygen stress response in *fc2* adult plants is blocked by the *pub4* mutation.

The effect of chloroplast $^1O_2$ accumulation was assessed in adult plants. (a) Four-week-old plants grown in constant (24h) light or under stressed conditions (three weeks in 24h light and one week in 16h light/8h dark diurnal (cycling) light conditions). (b) Representative rosette leaves (#'s 3 and 4) from the plants in (a). (c) Representative leaves (#'s 3 and 4) of plants after two and seven days of cycling light conditions, stained with trypan blue. The deep dark color is indicative of cell death. (d) and (e) show mean values (± SEM) of the trypan blue signal in leaves shown in (c) (n ≥ 6 leaves from separate plants). (f) shows the mean total leaf area (±SEM) of plants in panel (a) (n = 3 plants). (g) Mean total chlorophyll content (mg/g FW) (+/- SEM) of adult plant leaves grown in 24h light conditions (n = 6 biological replicates). For panels d, e, and g, statistical analyses were performed by a one-way ANOVA test followed by Tukey's HSD. Letters indicate statistically significant differences between samples ($P \leq 0.05$). For panel f, a two-way ANOVA followed by Sidak multiple comparison test were used for statistical analysis (n = 3 leaves from separate plants) (***, P value ≤ 0.001). Closed circles represent individual data points.

Figure 2: Photo-oxidative stress in *fc2* leads to a global change in transcript levels that is mostly reversed by the *pub4* mutation.

An RNA-Seq analysis was performed to measure steady-state transcript levels in plants grown in permissive constant (24h) light conditions for 19 days or 17 days in constant light conditions and shifted to singlet oxygen ($^1O_2$)-producing 16h light/8h dark diurnal (cycling) light conditions for two days. (a) A heatmap representation of the 1682 differentially expressed genes (DEGs) identified by at least one pairwise comparison between genotypes (*fc2* vs. wt or *fc2 pub4* vs. wt) in one condition (24h or cycling) that passed the applied cutoff values (Log_2FC > +/- 1.5

and a P*adj* < 0.01). The z-score color bar at the bottom shows the range of expression values, from decreased expression (blue) to increased expression (red). Genes are hierarchically clustered based on Euclidian distance of Log_2FC and complete linkage. (b) and (c) Venn diagrams depicting unique and shared up-regulated and down-regulated DEGs in 24h light and cycling light conditions, respectively.

Figure 3: Gene ontology enrichment analysis of differentially expressed genes in *fc2*.

Gene ontology (GO) term enrichment analyses of the identified (a) up- and (b) down-regulated differentially expressed genes (DEGs) in *fc2* mutants (compared to wt) in 16h light/8h dark diurnal (cycling) light conditions. Expression data is from the DESeq2 analysis of the included RNA-seq data set. GO-term enrichment analyses were performed using ShinyGO 0.80 with an FDR cutoff off of $p \leq 0.01$. x-axes indicate fold-enrichment. The ball size indicates the number of genes. The line colors represent FDR values. Shown are heatmaps representing the expression of (c) inducible and (d) repressible core singlet oxygen ($^1O_2$) response genes from the pairwise analyses "wt vs. *fc2*" and "wt vs. *fc2 pub4*" under cycling or constant light (24h) conditions. The z-score bar at the right shows the range of expression values, from decreased expression (blue) to increased expression (red).

Figure 4: Analysis of plastid protein-encoding gene expression during singlet oxygen stress

We assessed the effect of singlet oxygen ($^1O_2$) signaling on the expression of plastid protein-encoding genes (PPEGs). Expression data is from the DESeq2 analysis of the included RNA-seq data set. (a) Heat map showing the expression of 1730 PPEGs (both plastid- and nuclear-encoded) in *fc2* and *fc2 pub4* (relative to wt), grown under constant light (24h) and 16h

light/8h dark diurnal (cycling) light conditions. The up-regulated genes are shown in yellow, the down-regulated genes in blue, and genes with no change in expression are shown in green. (b) Pie chart showing the same 1730 PPEGs differentially expressed in wt vs. *fc2* (top) and wt vs. *fc2 pub4* (bottom), in cycling light conditions (*padj* < 0.01). The up-regulated genes are shown in yellow, the down-regulated genes in blue, and genes with no significant change in expression are shown in green. (c) Volcano plot representation of PPEG expression in *fc2* compared to wt, grown in cycling light conditions. The genes are color coded-based on the predicted localization of their protein products (thylakoid, envelope membranes, plastoglobules, and stroma with other associated locations). The x- and y-axes show $\log_2$ fold-change in expression and the Log_{10} false discovery rate of a transcript being differentially expressed, respectively. (d) Bar graph showing percentage of PPEGs that are up-regulated (yellow), down-regulated (blue), or have no significant change (green) in *fc2* in cycling light conditions (compared to wt), based on predicted sub-plastid localization of their protein products (envelope membranes, thylakoid, stroma, plastoglobule, ribosome, nucleoid, and unspecified locations within plastid) (*padj* < 0.01). (e) Venn diagram comparing differentially expressed PPEGs in *fc2* and *fc2 pub4*, in cycling light conditions compared to wt (*padj* < 0.01). The total gene counts are grouped as up-regulated or down-regulated, indicated by a red or blue arrow, respectively. Immunoblot analysis of selected plastid-encoded proteins (f) RBCL, (g) PsaA, and (h) PsbD from leaves of three-week-old plants grown in constant (24h) light conditions or grown in 24h light conditions and shifted to 16h light/8h dark diurnal (cycling) light conditions for two days. Shown are mean values compared to actin levels (+/- SEM) and normalized to wt in 24h light conditions (n ≥ 3 leaves from separate plants). Statistical analyses were performed using one-way ANOVA tests, and the different letters above the bars indicate significant differences within data sets determined by

Tukey-Kramer post-tests ($P \leq 0.05$). Separate analyses were performed for the different light conditions, and the significance of the cycling light is denoted by letters with a prime symbol (′). Statistical analyses of genotypes between conditions were performed by student's t-tests (*, $P \leq 0.05$; ns, $P \geq 0.05$). Closed circles indicate individual data points.

Figure 5: Activation of senescence pathways is blocked by the *pub4* mutation.

Senescence is induced in *fc2* mutants under cycling light conditions and blocked by the *pub4* mutation. (a) Expression data from the DESeq2 analysis of the included RNA-seq data set was used to create a heatmap of genes associated with senescence. Increased and decreased expression relative to wt is indicated by yellow and green, respectively. (b) Representative images of detached 3rd and 4th rosette leaves from plants grown in constant (24h) light conditions. The leaves were incubated in the dark with water (control conditions) or with 100 μM methyl jasmonate (MeJA) for 3 days. (c) Measurement of the maximum quantum efficiency of photosystem II (F_v/F_m) of leaves in panel b. (d) Total chlorophyll content of leaves in panel b. Statistical analyses were performed using one-way ANOVA tests, and the different letters above the bars indicate significant differences within data sets determined by Tukey-Kramer post-tests ($P \leq 0.05$). Separate analyses were performed for the different treatments, and the significance of the MeJA treatment is denoted by letters with a prime symbol (′). Statistical analyses of genotypes between conditions were performed by student's t-tests (*, $P \leq 0.05$; **, $P \leq 0.01$; ns, $P \geq 0.05$). n = 3 whole leaves from separate plants. Error bars = +/- SEM. Closed circles indicate individual data points.

Figure 6: Jasmonic acid biosynthesis and signaling are induced in *fc2* under cycling light conditions.

The impact of singlet oxygen ($^1O_2$) on jasmonic acid (JA) biosynthesis and signaling was assessed in constant light (24h) and 16h light/8h dark diurnal (cycling) light conditions. (a) Schematic illustration of the JA biosynthesis pathway, with relative expression (compared to wt in the same light condition) of 11 key JA biosynthesis and signaling genes. Expression data is from the DESeq2 analysis of the included RNA-seq data set. Error bars in the graph represent standard error (ifcSE) estimated by DESeq2 (**, *padj* < 0.01; ***, *padj* < 0.001). In chloroplasts, Defective In Anther Dehiscence 1 (DAD1) catalyzes the conversion of galactolipids into α-linolenic acid (α-LeA), which is converted into 12-oxo-phytodienoic acid (OPDA) by a series of enzymes; 13-Lipoxygenase (LOX), Allene Oxide Synthase (AOS), and Allene Oxide Cyclase (AOC). Subsequently, OPDA is exported out of the chloroplast via the channel protein JASSY. Inside the peroxisome, OPDA is reduced by the OPDA reductase 3 (OPR3) and shortened in the carboxylic acid side chain by β-oxidation enzymes (ACX1) into JA. In the cytosol, Jasmonate Resistant 1 (JAR1) conjugates isoleucine to JA converting it into JA-Ile. Jasmonate Transporter 1 (JAT1) transports JA-Ile into the nucleus. In response to stressed conditions, JA-Ile attach with the COI1-SCF (coronatine insensitive1- Skp1-Cul1-F-box), to promote ubiquitination and degradation of jasmonic acid repressors JAZ and JAV1, thereby activating JA response genes. (b) Graph showing JA content (ng/g fresh weight (FW)) measured in whole rosettes from plants grown for 19 days constant (24h) light conditions or 17 days in 24h light conditions and two days of 16h light/8h dark diurnal (cycling) light conditions. Values are means ± SEM (n = 3 biological replicates). Statistical analyses in b were performed using one-way ANOVA tests, and the different letters above the bars indicate significant differences within data sets determined by

Tukey-Kramer post-tests ($P \leq 0.05$). Separate analyses were performed for the different light treatments, and the significance of cycling light treatment is denoted by letters with a prime symbol (′). (c) Heatmap showing relative expression of 58 genes from gene ontology term "JA mediated signaling pathway" (GO:0009867). The blue and red colors correspond to low and high gene expression, respectively.

Figure 7: Blocking jasmonic acid synthesis does not strongly affect singlet oxygen-induced phenotypes in *fc2* mutants.

The *aos* mutation was tested for its ability to suppress $^1O_2$-induced cell death in *fc2*. (a) Representative images of seven-day-old seedlings, grown in constant (24h) light conditions or 6h light/18h dark diurnal (short day) light conditions, and stained with trypan blue. The dark blue color is indicative of cell death. (b) Quantification of cell death measured in seedlings grown in short-day conditions in panel a. Shown are mean values +/- SEM of the trypan blue signal ($n \geq 8$ seedlings). (c) Representative images of plants grown in 24h light conditions for four weeks or 24h light conditions for three weeks and cycling light (16h light/8h dark) conditions for one week. Quantification of (d) total leaf area, (e) fresh and (f) dry weight biomass from plants grown in 24h light in panel c. Shown are mean values ± SEM ($n = 3$ plants). Quantification of (g) total leaf area, (h) fresh and (i) dry weight biomass from plants grown in cycling light in panel c. Shown are mean values ± SEM ($n = 3$ plants). All the statistical analysis was performed by one-way ANOVA followed by Tukey's multiple comparison test. Different letters above the bars indicate significant differences (P value ≤ 0.05). Closed circles represent individual data points.

Figure 8: Singlet oxygen and *pub4* alter the expression of Salicylic acid-related genes and Salicylic acid content.

The effect of singlet oxygen ($^1O_2$) on Salicylic acid (SA) content and signaling was assessed. (a) An overview of SA synthesis via the isochorismate synthesis (ICS) (left side) and the phenylalanine ammonia-lyase (PAL) pathway (right side). (b) Relative expression (compared to wt in the same light condition) of ten key SA biosynthesis genes from panel a. Genes involved in the ICS and PAL pathways are labeled in yellow and blue, respectively. Expression data is from the DESeq2 analysis of the included RNA-seq data set. Error bars in the graph represent standard error (ifcSE) estimated by DESeq2 (*, *padj* < 0.01). (c) Heatmap showing relative expression of genes associated with the regulation of SA biosynthesis from the RNA-seq data set ("wt. vs. *fc2*" or "wt vs. *fc2 pub4*" in constant 24h light conditions or after two days of 16h light/8h dark diurnal (cycling) light conditions). The blue and red colors correspond to low and high gene expression, respectively. (d) SA content (ng/g fresh weight (FW)) measured in 17-day-old plants (grown in 24h light conditions or after two days of cycling light conditions). Shown are mean values ± SEM (n = 3 replicates). Statistical analysis was performed by one-way ANOVA followed by Tukey's multiple comparison test. Different letters above the bars indicate significant differences (*P* value ≤ 0.05). Closed circles represent individual data points.

Figure 9: Blocking Salicylic acid in *fc2* mutants impairs light stress tolerance.

The effect of blocking Salicylic acid (SA) synthesis in the *fc2* mutant with the *esd16* mutation was evaluated. (a) SA and (b) Jasmonic acid (JA) content (ng/g fresh weight (FW)) were measured in whole rosettes from plants grown in constant (24h) light conditions for 17 days and then two days of 16h light/8h dark diurnal (cycling) light conditions (n = 3 biological

replicates). (c) Representative images of plants grown in 24h light conditions for four weeks or in 24h light conditions for three weeks before a light shift (LS) (plants were subjected to ~4 μmol photons s^{-1} m^{-2} for 8 hours and then shifted back to ~120 μmol photons s^{-1} m^{-2} light for 5 days). (d) Representative images of leaves (numbers 5 and 6) from plants grown under 24h light conditions, 24h light conditions followed by two days of cycling light conditions, or after a light shift and stained with trypan blue. The dark blue color is indicative of cell death. (e) and (f) Fresh weight (FW) and dry weight (DW) of plants grown in 24h light conditions ($n \geq 5$). (g) Quantification of the trypan blue signal in leaves from plants grown in cycling light conditions ($n \geq 9$ individual leaves from separate plants). (h) A schematic diagram illustrating the experimental setup for growing plants in 24h light, cycling light, and light shift (LS) conditions. (i) Quantification of the trypan blue signal in leaves from plants grown in LS conditions ($n \geq 8$ individual leaves from separate plants). (j) and (k) FW and DW of plants grown in LS conditions ($n = 6$). Mean values (+/- SEM) are shown in all graphs. All the statistical analyses were performed by one-way ANOVA followed by Tukey's multiple comparison test. Different letters above bars indicate significant differences (P value ≤ 0.05). Closed circle represents individual data points.

Figure 10: <u>The *eds16* mutation reverses the *pub4* phenotypes during singlet oxygen stress.</u>

The effect of the *eds16* mutation on *fc2 pub4* was assessed. (a) Shown are representative images of seven-day-old seedlings, grown in constant light (24h) and 6h light/18h dark diurnal (cycling) light conditions stained with trypan blue. The dark blue color is indicative of cell death. (b) Mean values (± SEM) of the trypan blue signal in seedlings from panel (a) ($n \geq 10$ seedlings). (c) Representative four-week-old plants grown in 24h constant light conditions. (d) Fresh weight

and (e) dry weight measurements (mean ± SEM, n ≥ 4 plants) of plants shown in panel (c). (f) Total chlorophyll content in whole rosettes of 4-week-old plants grown in constant light conditions (mean ± SEM, n ≥ 3 plants). (g) Representative images of leaves (numbers 5 and 6) from plants grown in 24h light for three weeks and then 16h light/8h dark diurnal (cycling) light conditions for seven days, stained with trypan blue. (h) Quantification of the trypan blue signal of leaves in panel (g) (mean ± SEM, n ≥ 7 individual leaves from separate plants). (i) Representative images of 21-day-old plants grown in 24h conditions and exposed to excess light (1,500 µmol photons m^{-2} sec^{-1}) for 24h at 10°C. White arrows indicate lesions. (j) Quantification of lesions from panel (i) (n ≥ 4 plants). Values are means (+/- SEM) of leaves with lesions / total leaves. Statistical analyses were performed by one-way ANOVA tests followed by Tukey's multiple comparison test. Different letters above the bars indicate significant differences (*P* value ≤ 0.05). Closed circle represents individual data points.

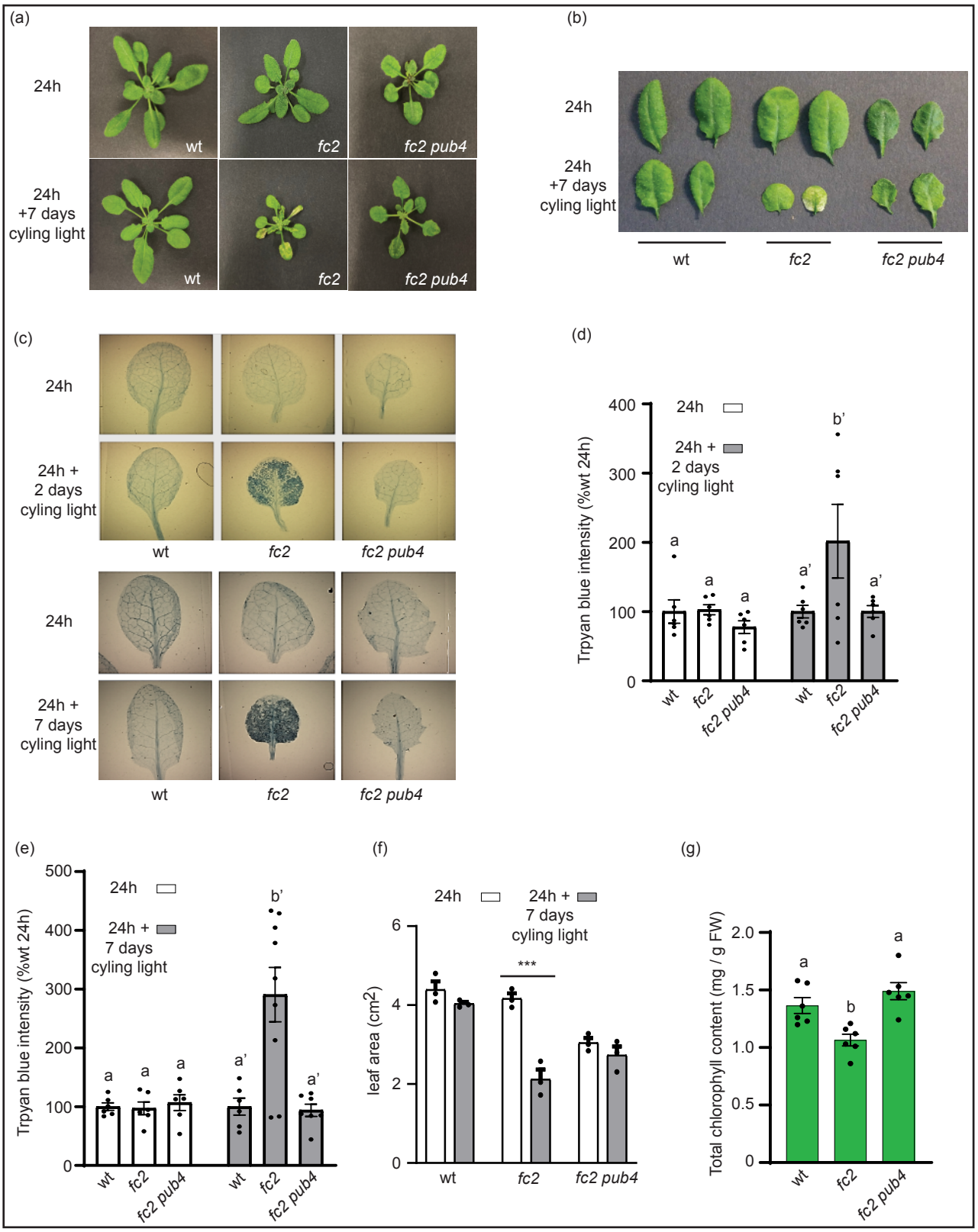

Rai *et al.* 2024 Figure 1

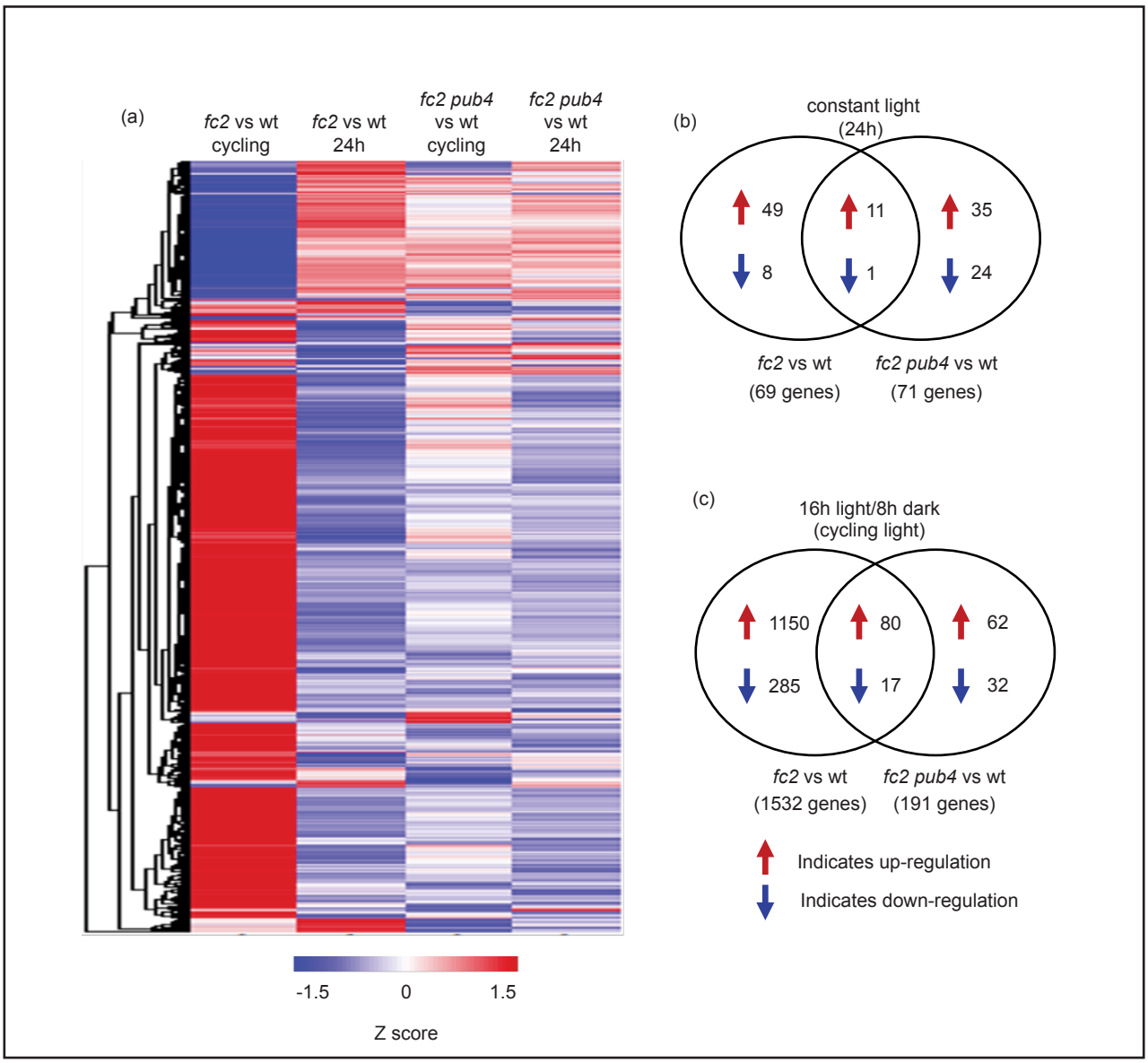

Rai *et al.* 2024 Figure 2

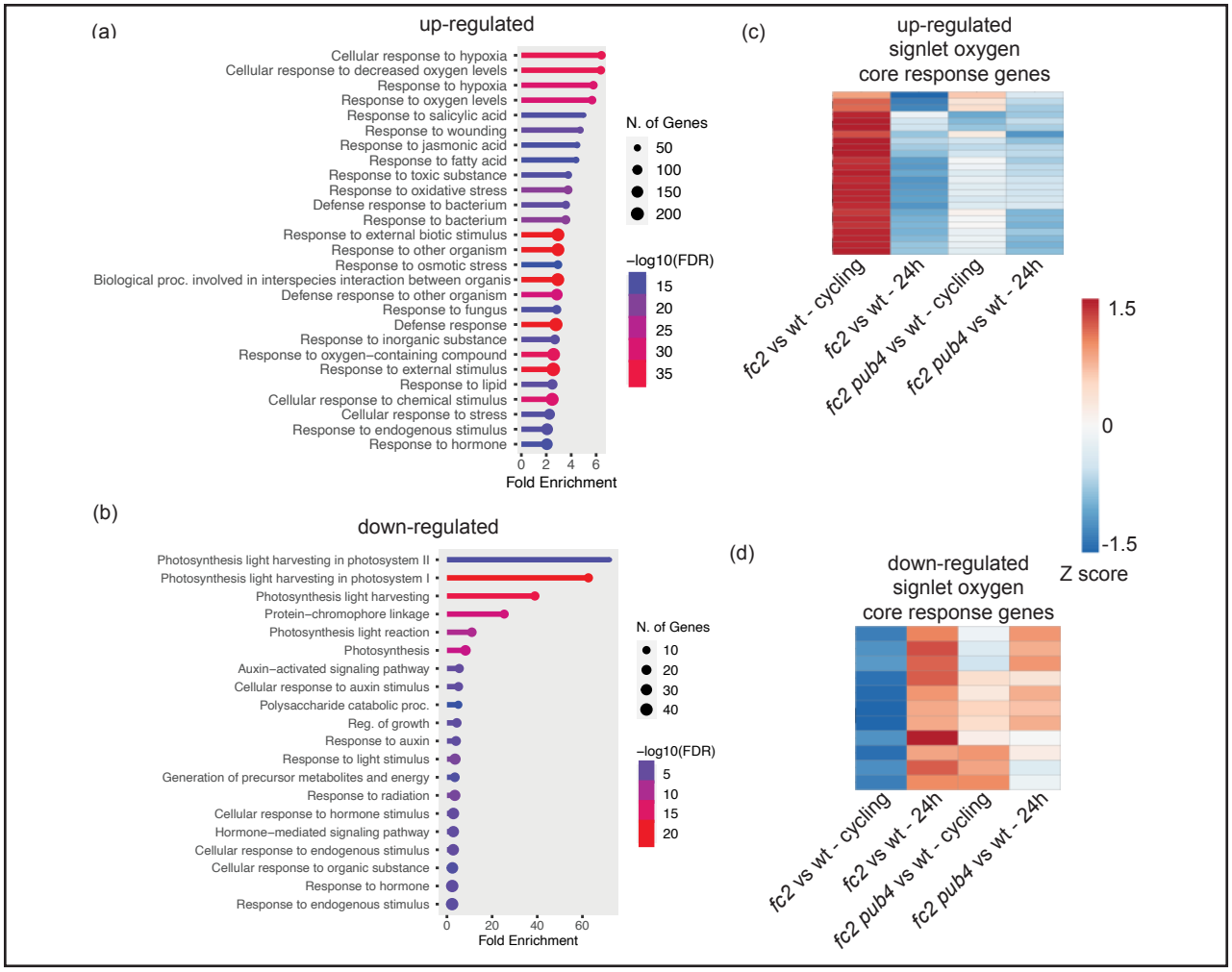

Rai *et al.* 2024 Figure 3

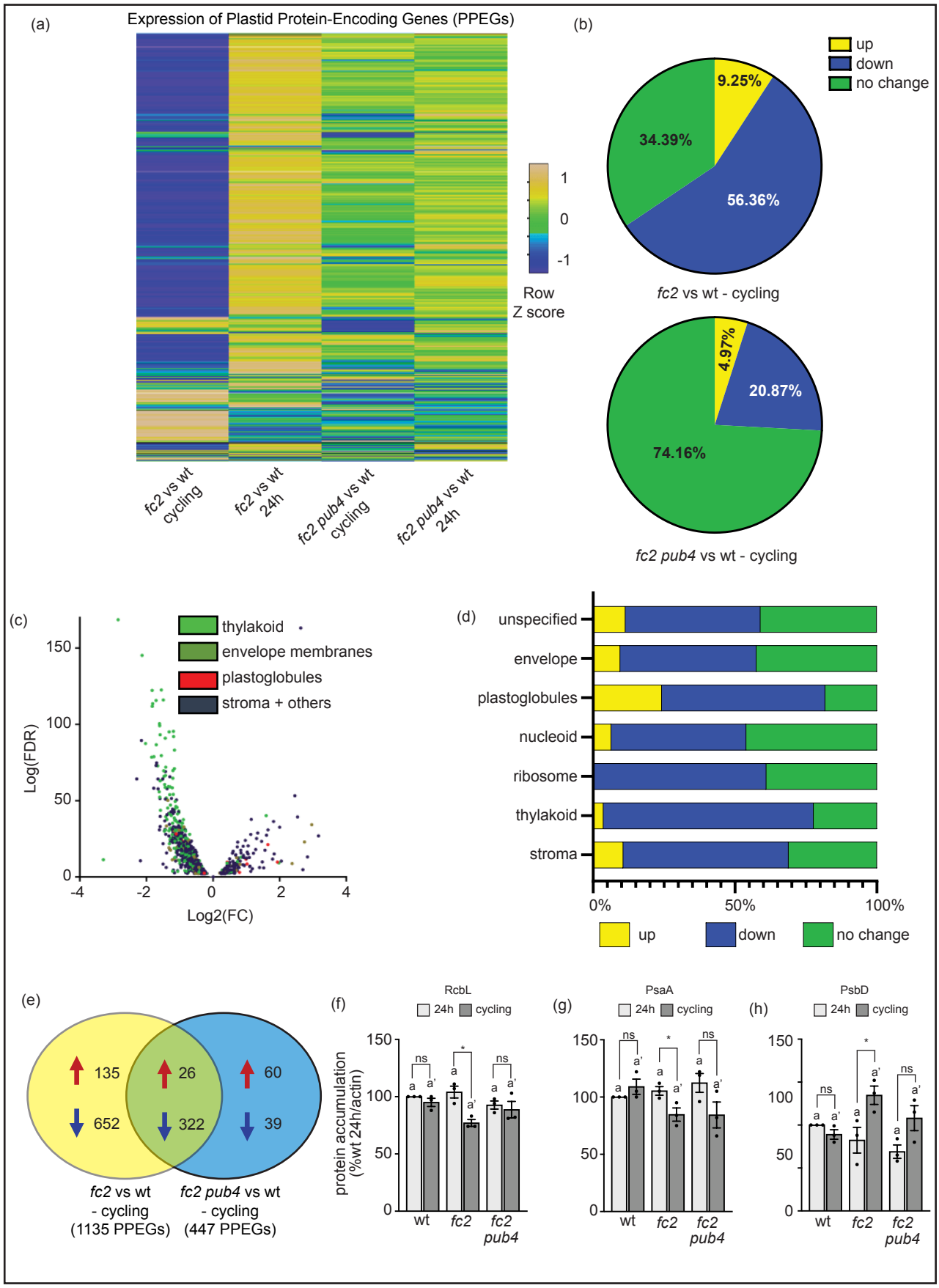

Rai *et al.* 2024 Figure 4

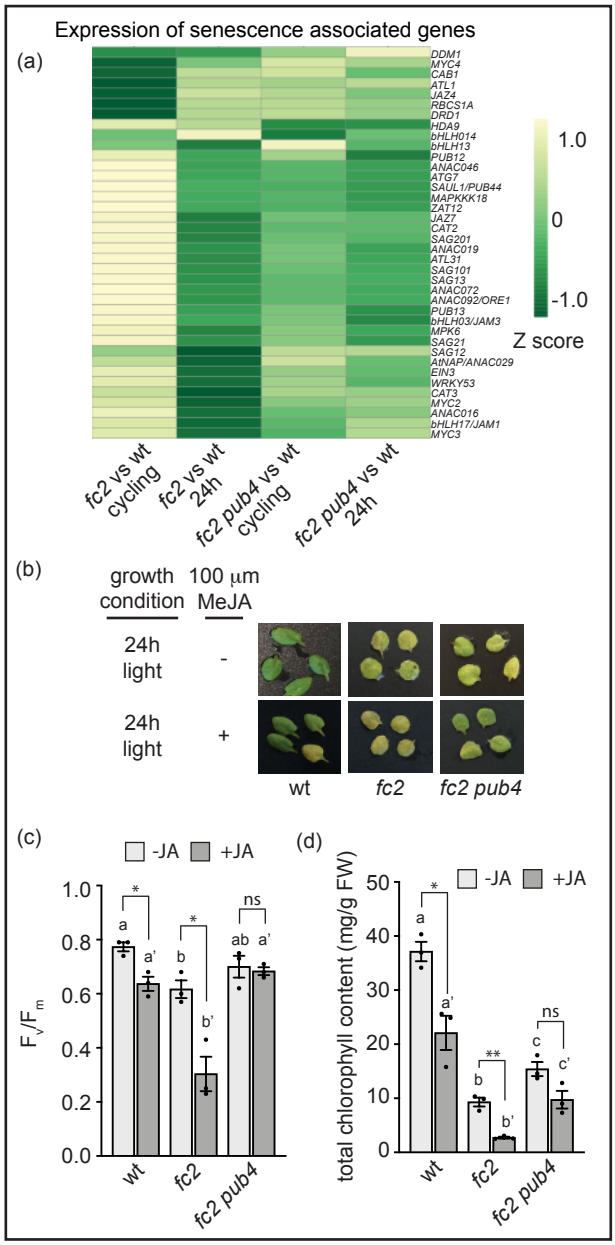

Rai *et al.* 2024 Figure 5

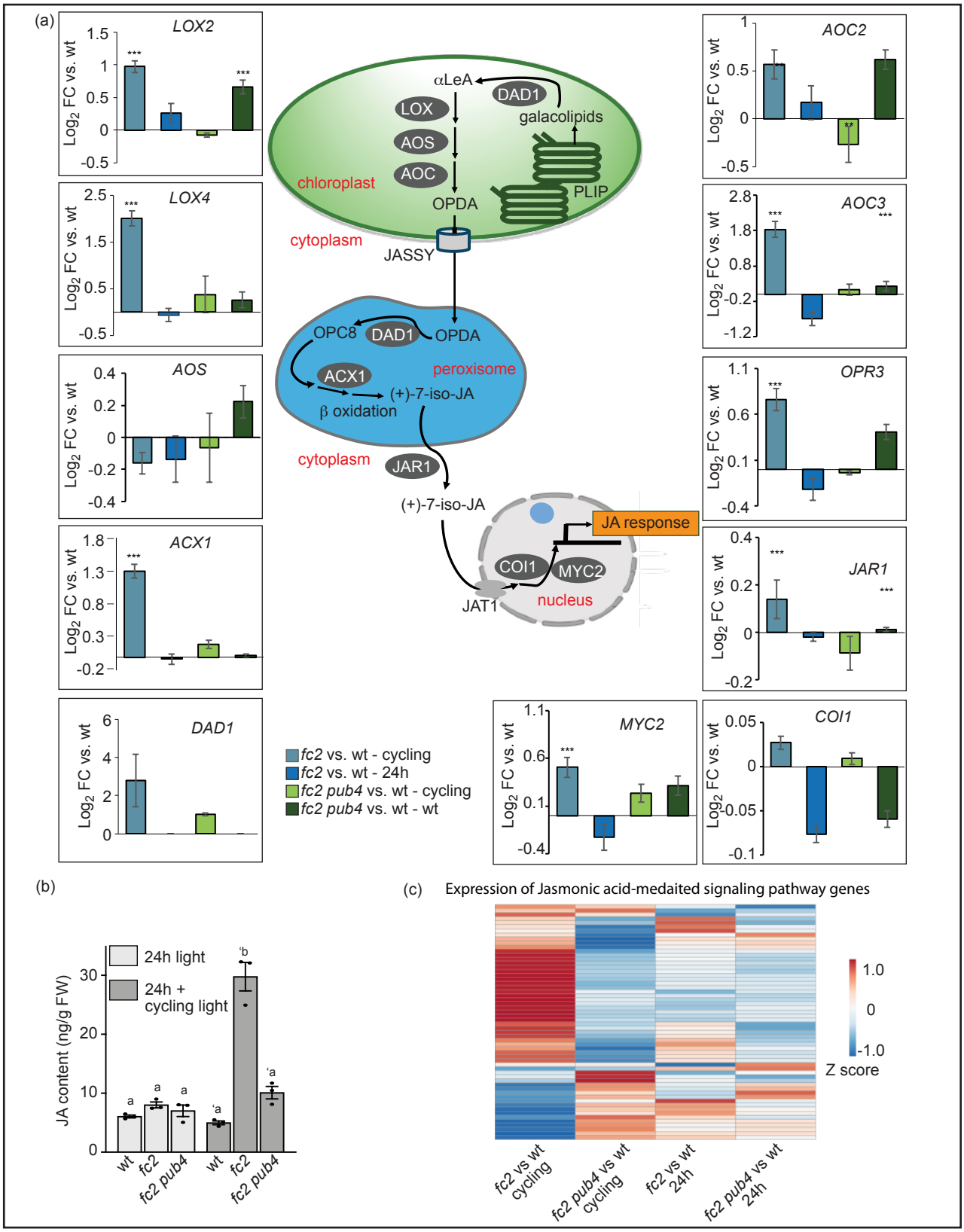

Rai *et al.* 2024 Figure 6

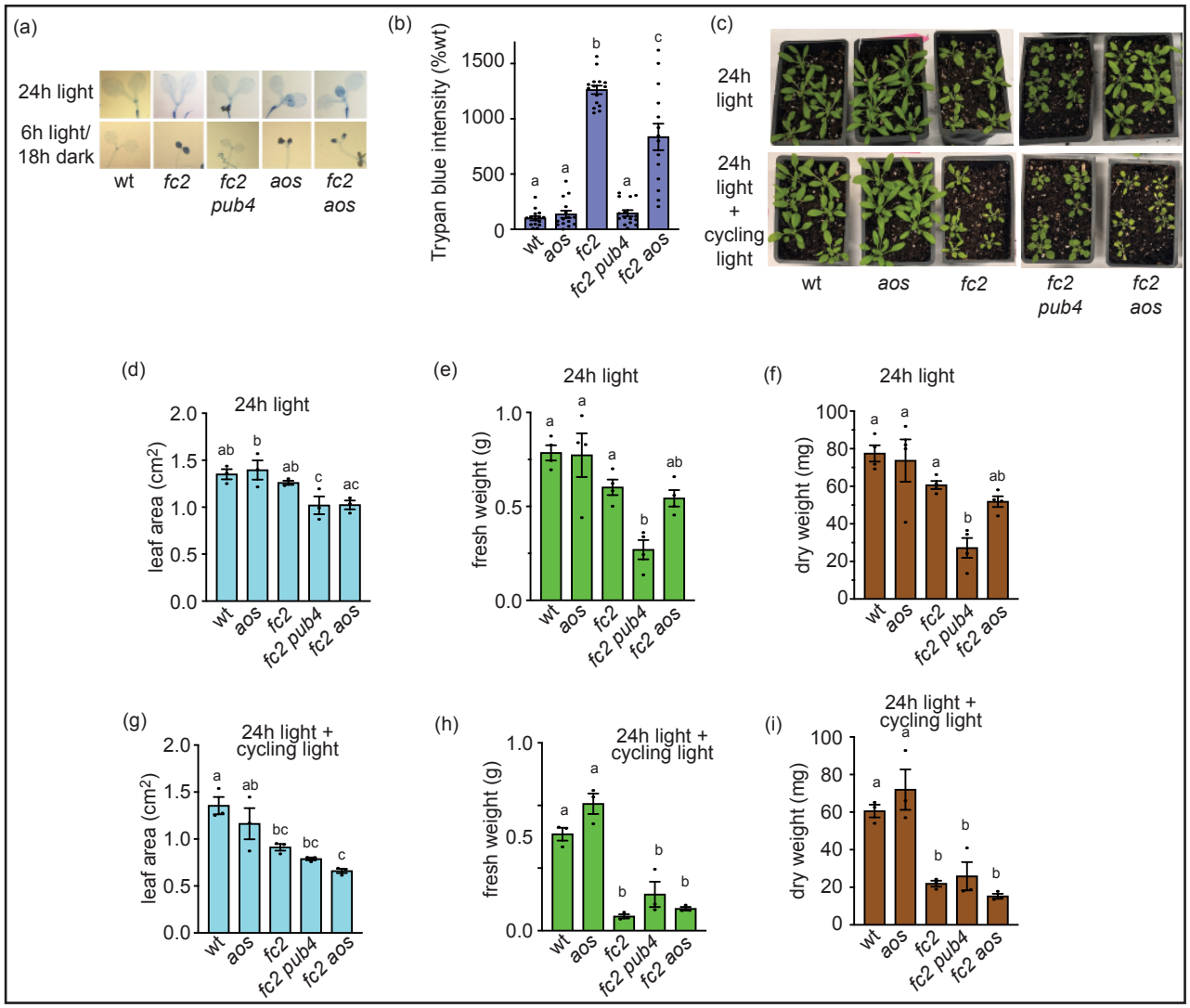

Rai *et al.* 2024 Figure 7

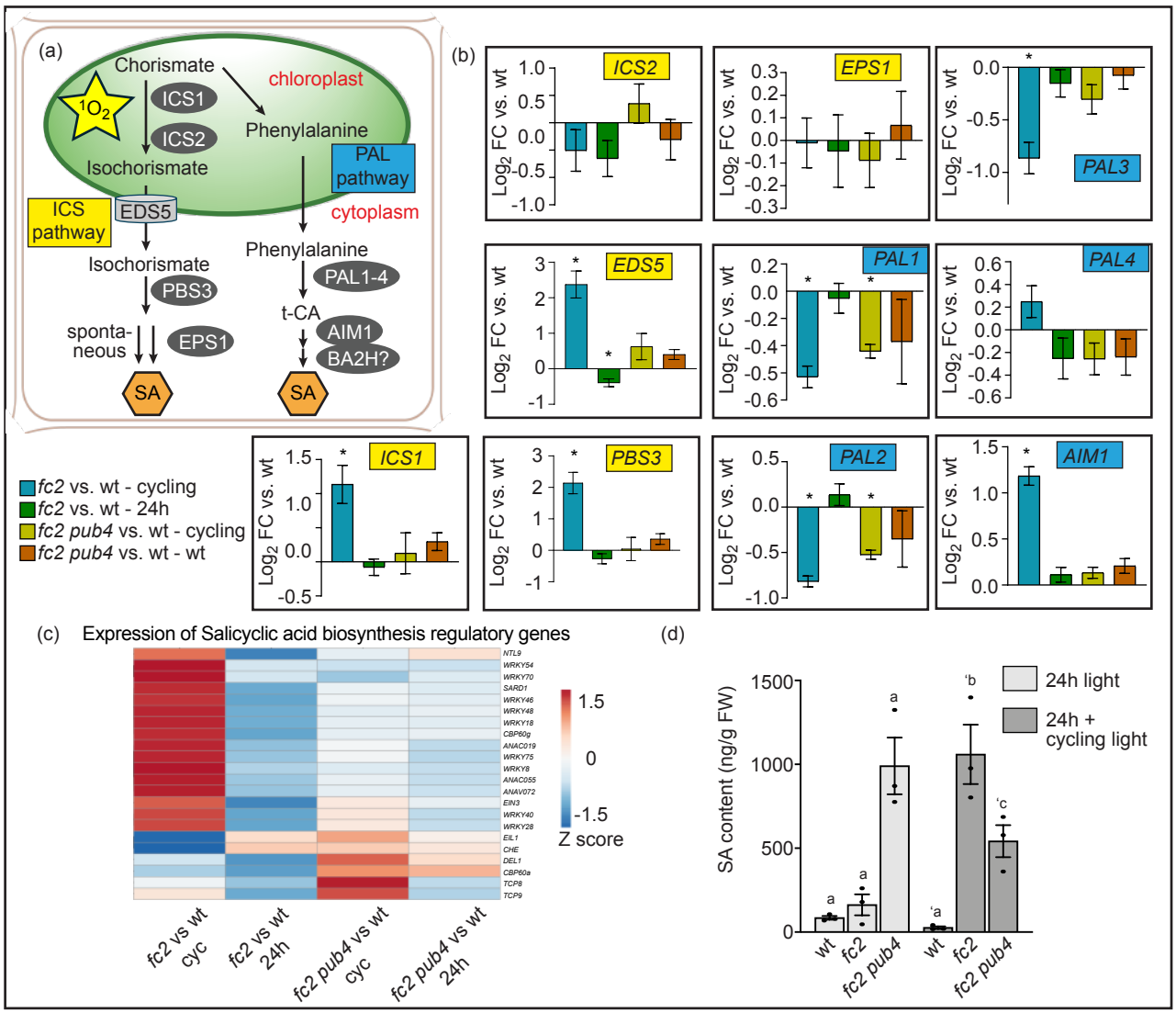

Rai *et al.* 2024 Figure 8

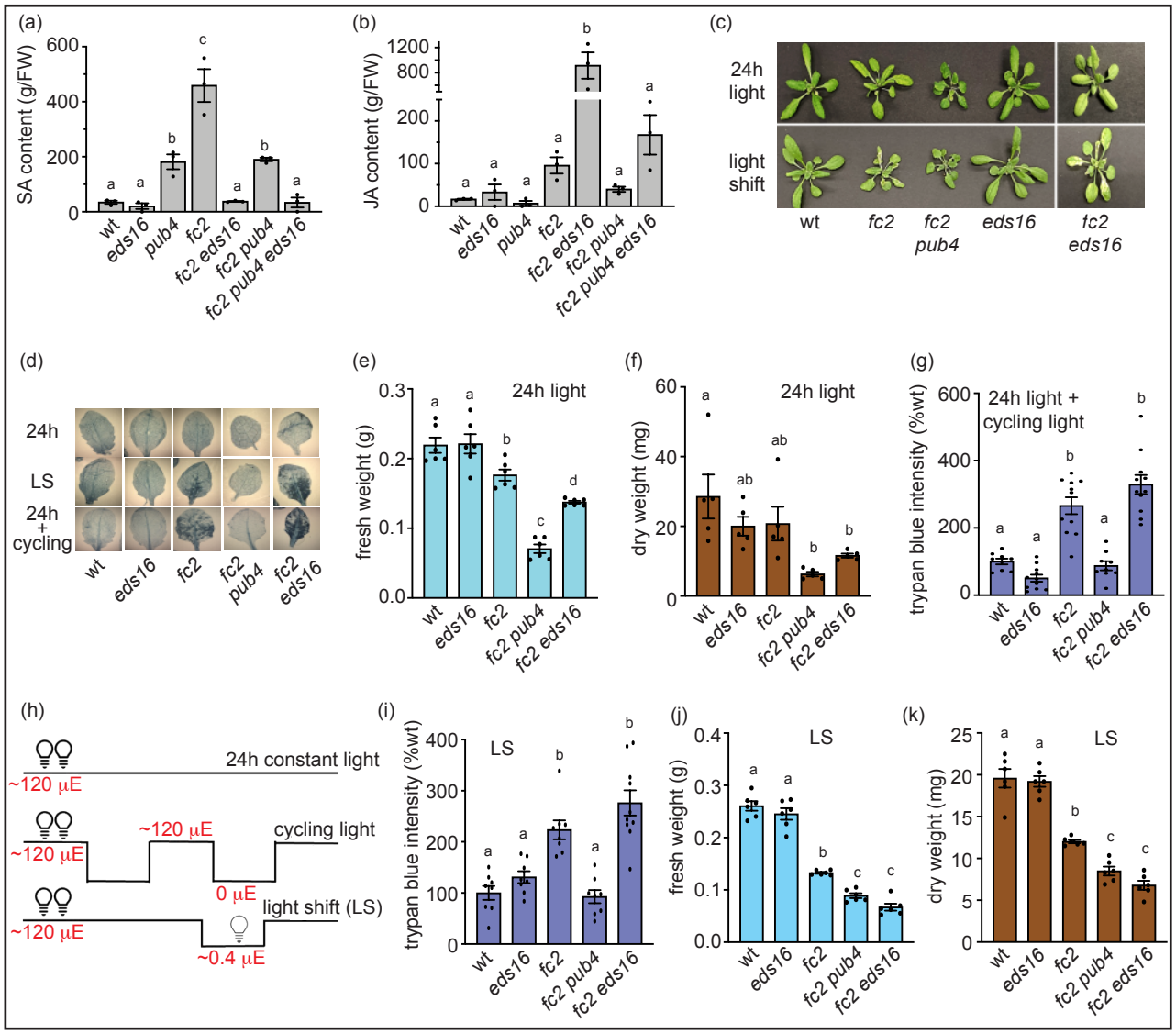

Rai *et al.* 2024 Figure 9

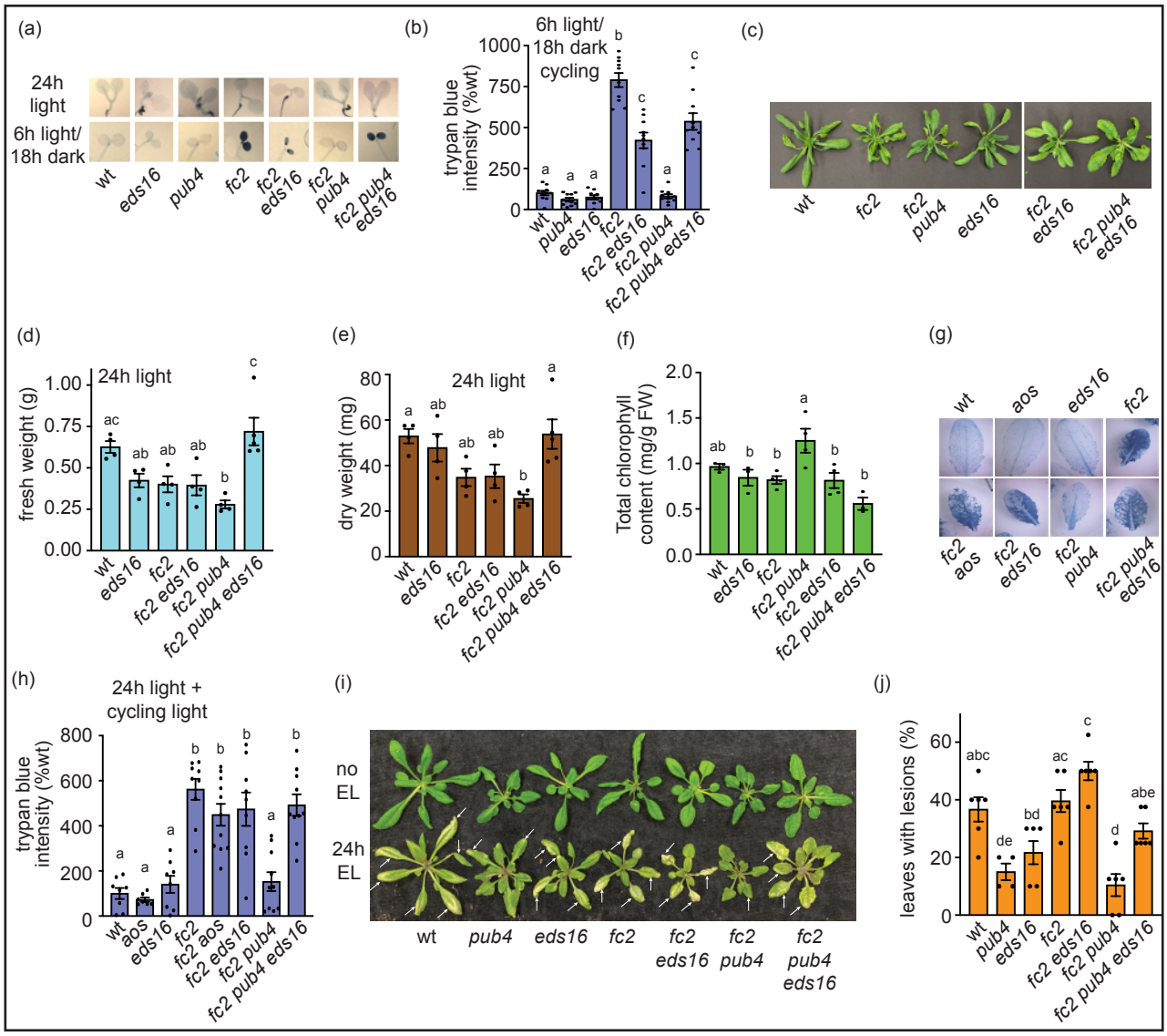

Rai *et al.* 2024 Figure 10